RADIOTHERAPY DOSE VERIFICATION OF PROSTATE TUMOURS BY USE OF MOTION CONTROLLED 3D RADIATION DOSIMETERS

Adrian Stephen Balatinac

Bachelor of Engineering
Mechanical Engineering Major

Department of Mechanical Engineering
Macquarie University

June 05, 2017

Supervisor: Prof. Yves De Deene

MACQUARIE UNIVERSITY

DEPARTMENT APPROVAL

of a senior thesis submitted by

Adrian Stephen Balatinac

This thesis has been reviewed by the research advisor, research coordinator, and department chair and has been found to be satisfactory.

Date	Supervisor: Prof. Yves De Deene, Advisor
Date	A, Research Coordinator
Date	B, Chair

ACKNOWLEDGMENTS

I would like to acknowledge my supervisor Prof. Yves De Deene for his encouragement, time, and guidance at every stage of my research. Thank you for pushing me to think critically and work independently. I would like to acknowledge and thank Masoud Toghyani, Stephen Balatinac, Dr Nicholas Tsang, and Anne-Marie Tsang for their guidance and support throughout.

STATEMENT OF CANDIDATE

I, Adrian Balatinac, declare that this report, submitted as part of the requirement for the award of Bachelor of Engineering in the Department of Mechanical Engineering, Macquarie University, is entirely my own work unless otherwise referenced or acknowledged. This document has not been submitted for qualification or assessment at any academic institution.

Student's Name: Adrian Stephen Balatinac

Student's Signature:

Date: 05/06/2017

ABSTRACT

With the increasing use of radiation treatments for patients with cancer, there has been a growing concern with the quality of the treatments. There may be errors in accuracy and dosage of the treatment that are not detected in the planning and delivery of the radiation. Until recently, in radiotherapy, the radiation beams were delivering radiation to a static target. In other words, the radiation target is considered not to move with respect to the radiation beams. However, certain tumours do move during the radiation treatment, especially lung tumours upon inspiration and expiration, and tumours in the abdomen as a result of normal bowel function.

With the many challenges that are present in radiotherapy, there is a growing need for the use of 3D radiation dosimeters, which upon being irradiated, change colour. This further extends to motion controlled 3D radiation dosimeters, which are used to mimic the movements of tumours during radiotherapy. This study investigates the dose verification of radiation applied to prostate tumours during standard radiotherapy, and aims to implement a radiation dosimetry technique that is able to measure the dose in three dimensions in a moving prostate dosimeter. The elastomer gel named FlexyDos3D was the substrate utilised for these experiments. Given the limiting stability of Flexdos3D this study further scrutinised this elastomer gel, through examining the potential evaporation of the initiator, and altering both the chemical composition and chemical concentrations of FlexyDos3D.

Contents

List of Figures

List of Tables

Chapter 1

Introduction

1.1 Project Objective

The aim of radiotherapy is to deliver a precise radiation dose to cancerous tissue, while minimising the dose to healthy surrounding tissue. However, the errors in the dosage and delivery of radiotherapy may not be detected in the planning stage. This study hopes to improve the quality assurance of image guided radiation therapy (IMGRT) of prostate tumours at the Royal North Shore Hospital (RNSH) by implementing and optimising an automated motion driven 3D radiation dosimeter. The short-term goal is to benchmark and validate the motion actuated 3D radiation dosimeter in terms of both dosimetric characteristics (stability, temperature sensitivity, etc.) and in terms of the reproducibility (shape) of the dosimeter. In the long run, the aim is to provide a standardised 3D dosimetry protocol for IMGRT to safeguard the radiotherapy treatment administered to cancerous tissue.

In recent years, greater attention has been directed towards utilising motion controlled 3D radiation dosimeters to ensure a more accurate dose delivery of radiation to cancerous cells. The 3D radiation dosimeters are composed of a silicon elastomer which, when exposed to radiation, changes colour. This change can then be quantified using an optical scanner. This study will be using the 3D radiation dosimeter, designed by the Macquarie University team, made from an elastomer gel named FlexyDos3D.

While the 3D dosimeter is being irradiated, a tracking device will be utilised to track the motion of the dosimeter. This will be conducted at the RNSH. The tracking technique intends to deliver a more precise dose of radiation, and hence sparing healthy surrounding tissue in the real world application. The dosimeter will be scanned using an optical scanner designed by the Macquarie University team. At the present moment, there are no techniques available to verify the accuracy of IMGRT in 3D.

In an effort to minimise errors or discrepancies, the stability of the FlexyDos3D was also investigated. An underlining issue remains with the chemical composition of FlexyDos3D, causing the dose distribution to slowly change over time, consequently affecting the reproducibility of the experiments. To examine and potentially improve this, several experiments were conducted. First, in an attempt to improve the stability of the 3D

dosimeter, chloroform will be replaced with dibromomethane as the initiator in FlexyDos3D. Secondly, the possible effect of evaporation of the initiator (chloroform) will be investigated, which changes the radiation dose distribution in the vicinity of irradiation. Thirdly, the effect of the elastomer resin and curing agent will be investigated. These initial studies are essential in providing a reliable 3D dosimeter for dose verification of prostate IMGRT.

To have an improved understanding of the properties of FlexyDos3D, an investigation was also initiated into determining its mechanical properties at its most suitable and stable chemical concentrations. Furthermore, in order to commence radiotherapy treatment on the 3D prostate tumour dosimeter, modelling and 3D printing of a prostate tumour mould for the FlexyDos3D elastomer gel was completed.

1.2 Deliverables

- Standardising the fabrication of 3D dosimeters in a reproducible way.
- A standardised procedure for obtaining the 3D dose distribution of dosimeters using an optical scanner. The results may then be further studied to improve the radiation treatment to patients.

Chapter 2

Background and Related Work

Radiation sensitive gels were first proposed by Day and Stein in 1950, which upon being irradiated would change colour. It was as early as 1954 when radiation dosimeters were first proposed, and a large amount of different types of gels and polymers have been designed since, such as the BANANA polymer gel dosimeter (1992), and BANG polymer gel dosimeter (1994). Since the development of these gel dosimeters, there has been greater attention applied into researching and utilising these dosimeters [3].

Researchers applied these dosimeters in intensity modulated radiation therapy (IMRT), intensity modulated arc therapy (IMAT), volumetric modulated arc therapy (VMAT), stereotactic radiosurgery, brachytherapy, low energy x-rays, and proton therapy. Researchers also begun into the clinical applications of the dosimeters using magnetic resonance imaging (MRI) [3].

In 2001, a significant step was made in designing a normoxic polymer gel dosimeter, which could be manufactured around oxygen. This was accomplished through adding an anti-oxidant into the composition. This new polymer gel dosimeter was named MAGIC, designed by Fong et al (2001) [4, 5]. Until then, the dosimeters were hypoxic, meaning they would undergo the premature polymerisation process in the presence of air when manufactured. Senden et al (2006) summarises the research done in further developing the modern normoxic gels [6].

2.1 Conformal Radiotherapy

Conformal radiation therapy (CRT), delivers radiation by the use of a dynamic multi-leaf collimator (DMLC). The DMLC works by the metal leafs conforming to the desired shape of the cancerous cells. The CRT delivers a precise radiation dose from multiple angles, minimising the radiation given to the healthy surrounding tissue. The focal point of the multiple radiation beams (the tumour) is subject to a higher radiation dose. In CRT, all the radiation beam parameters must be set manually, where the beams can only be set to one strength. [7]

Image guided radiation therapy utilises various imaging modalities unto the linear accelerator (the radiation source) [8]. These most typically are ultrasound, 2D X-ray, and

computed tomography [8]. The imaging techniques provide information in identifying where the radiation source is aimed relative to the patient, and subsequently the tumour. They may be used to provide cross sectional imaging, or even rotated 360^o around the patient feeding back real time images in three dimensions. This therapy was specifically designed for delivering more precise radiation in applications where a patient cannot lie still, or where a tumour is moving due to normal organ functions.

Intensity modulated radiation therapy is similar to that of CRT, where multiple radiation beams are focussed on cancerous cells. IMRT uses a multi-leaf collimator to deliver precise radiation, with the added advantage of modulating and controlling the intensity of the radiation beams, unlike CRT. [7, 9]

2.2 Dosimeter Types

The move from hypoxic polymer gels to normoxic has not only ceased the polymerisation process in the presence of air, but has allowed the fabrication process to be significantly easier. There are four categories that a 3D dosimeter composition falls under. These are:

- *Polymer Gel* - A gelatine hydrogel with vinyl monomers and anti-oxidant [1, 3]. Most suitable with MRI, Optical Computerised Tomography (CT), and X-Ray CT.
- *Fricke Gel* - Also known as Fricke Xynlenol Gel (FXG), is composed of ferrous ions with the metal ion indicator xylenol-orange, in an acidic gel. Most suitable with optical CT. [10]
- *Plastic* - Uses a polymer matrix instead of a hydrogel, such as polyurethane. Suitable only with optical scanners
- *Elastomer Gel* - An amorphous polymer, such as polydimethylsiloxane silicones (PDMS). Suitable only with optical scanners.

When using elastomer gel dosimeters in radiotherapy, it is important to both fabricate and irradiate the dosimeter and calibration samples from the same batch. This is to minimise any discrepancies between the two [11]. The advantage of using elastomer gels over others types, is their ability to be poured into anthropomorphic shaped moulds such as organ casts. These may be used in motion controlled 3D dosimeters. [9]

The fabrication temperature and storage of the gels are vital factors to be considered. Exposure to any ultraviolet (UV) source, such as sunlight, may trigger the gel to respond. Storage for the gels then must be in a dark location. Hanif (2016) studied the different temperatures at which storage for the elastomer is ideal. The storage temperatures before irradiation played a small factor on the elastomers response compared to the storage temperatures post irradiation. It was found that the colder the storage temperature, the more stable the response was over time. The stability still slowly degrades, but at a far slower rate than when stored at room temperatures. [12]

More recently designed gels are found to be less toxic, or not toxic at all [3]. Unfortunately, the majority of the designed gels do not suit the application of a motion controlled 3D dosimeter. De Deene (2014) recently designed an elastomer based 3D dosimeter named FlexyDos3D. The elastomer gel is flexible and strong, consisting of transparent polydimethyl siloxane elastomer. The radiation activated chemical is Leuco Malachite Green (LMG) [1]. It satisfies the 3D dosimeter characteristics, along with excelling in tissue equivalence to cancerous tissue and spatial integrity. FlexyDos3D is also non-toxic.

2.3 Irradiation

Upon the FlexyDos3D elastomer gel being irradiated, a chemical reaction occurs where the LMG is converted into a coloured form [13]. The colour change is proportional to the radiation dose; changing from transparent to a tinted green in FlexyDos3D. Polymer gels are slightly different to elastomers, as they undergo a property change referred to as nuclear magnetic resonance (NMR) spin-spin relaxation rate (R_2). This is what determines the amount of polymerisation [1]. There have been a few studies on the different sources of radiation given to the dosimeters, where the most common are gamma rays from a cobalt source and high energy X-rays from a linear accelerator. However, if these dosimeters are to one day be utilised in radiotherapy, it remains important that the radiation dose given to the dosimeter is the same as that given to a patient during treatment. [3]

Earlier studies have shown that the chemical response of the FlexyDos3D is similar when exposed to UV radiation as compared to ionising radiation [14]. High-energy X-rays are only available in the hospital, and requires the engagement of staff after normal working hours. It was found more convenient to perform experiments with UV radiation.

2.4 Imaging

The three most common imaging techniques used to read the dose distribution are MRI, optical CT, and X-ray CT [3]. The change in the NMR of the polymer gel dosimeter allows an MRI to identify the dose distribution [1]. However, an issue may arise with the limitation of gaining access to an MRI machine. They are not only costly, but there is also limited availability to use an MRI. Much expertise is also required to obtain accurate quantitative R_2 maps. Similar issues may arise with utilising optical CT and X-ray CT machines. For these reasons, more research is being conducted into not being reliant on MRI, Optical CT, and X-ray CT.

The use of an optical scanner is less costly, and does not require professionally trained personnel to operate. An issue arises with the scattering of light within polymer gels when using an optical scanner, leading to artefacts and uncertainties in the dose distribution [1]. FlexyDos3D does not have this issue, as it is an elastomer gel.

There have been several types of optical scanners through the years. The first optical CT scanner was developed by Gore et al (1996) [15]. It involved a laser scanning across one dimension, at each increment the sample was rotated [3]. Since this development, the

technology for more efficient and accurate optical scanners have evolved. One particular design was named OCTOPUS by MGS Inc. [3]. A large factor that has driven further development into optical CT scanners, was the slow time to complete scans. OCTOPUS takes approximately 12 minutes to process one slice at an image of 128x128 pixels. The process would consequently take many hours to scan a full 3D sample in high resolution [3]. Since then, developments have progressed to the proposal of using a cone-beam configuration [16]. This scanner uses pixelated area detectors to capture a 2D projection. The time to complete this would take only minutes. A similar device is named VISTA, developed by Modus Medical Devices Inc [2,3].

Until recently, Macquarie University has used a parallel beam configuration which was first proposed by Doran et al (2001) [3,17]. This uses a laser beam to be reflected off an galvano-mirror. The mirror is rotated precisely, allowing the laser to sweep across, and fall unto a convex lens. The convex lens ensures the beams follow parallel paths through the sample. The beams leaving the sample, fall onto a photo-diode which measures the transmitted light [1].

Currently, the optical CT scanner at Macquarie University utilises a cone beam based on the Modus Vista scanner to scan an object in high resolution [13]. The scanner works by utilising a charge coupled device (CCD) camera, pinhole, and a back projection as seen in figure 2.1 [2]. The dosimeter is suspended from above in a holder, which is in glycerol fluid. The glycerol fluid has a refractive index similar to that of the dosimeter, avoiding any deflections of light which hit the dosimeter [1]. The scanner utilises a dual wavelength scanning method, where the dosimeter is scanned first using a blue light (630nm), then a red light (400nm). With this method, the need to reposition the dosimeter is avoided, minimising the chance of artefacts and errors [1]. The dosimeter only absorbs light around 630nm, and so to determine the optical density of the dosimeter, the optical density of the blue light is subtracted from the red. This is shown in the equation 3.1. Optical density does not depend on the density of the material, instead corresponds to the absorbed light at a corresponding wavelength. It may be measured by an optical CT scanner or a spectrophotometer, and is unit-less.

The dosimeter within the scanner rotates at each angular increment, while the CCD records the images at each degree [1]. The convergence of light through the pinhole is also taken into account. This entire scan takes less than 10 minutes, and allows the use of non-cylindrical dosimeters to be scanned.

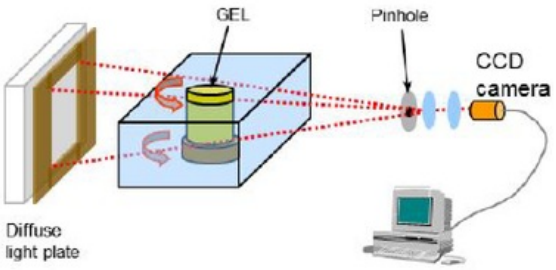

Figure 2.1: *Diagram of the cone beam optical CT scanner. This system utilises a dual wavelength technique, which allows non cylindrical dosimeters to be scanned without the need to be repositioned. Light that is transmitted by the diffuse light plate passes through the dosimeter, and is picked up by the CCD camera at every incremental rotation. The images are reconstructed using MATLAB, taking into account the convergence of the beam. [1, 2]*

2.5 Motion Controlled 3D Dosimeters and Tumour Tracking

Optical scanning of non-cylindrical dosimeters has opened doors for new applications. The new technology developed has enabled radiotherapy techniques to now track the motion of a tumour undergoing treatment. There is a growing need for motion controlled deformable dosimeters to verify that the techniques are accurate. Yeo et al (2012) investigated a tool for the design of a deformable gel dosimeter, named DEFGEL, to mimic the deformation in different states [18]. With this, the study of measuring and verifying radiation doses in motion and deformable states became possible.

With the concern on the quality of treatment, there is a rising need for planning and delivering accurate radiation doses. To ensure that the correct amount of radiation is given, at the right place, 3D dosimeters are used along with motion tracking. Until now, radiation has been given on a static target, meaning the target did not move when undergoing treatment. However, this isnt always the case. Certain tumours that are located on organs, such as the lungs or bowel, do move. This is problematic as the radiation may not hit only the tumour, but healthy surrounding tissue.

De Deene (2014) placed a prostate tumour motion controlled 3D dosimeter into a pelvic phantom, and while the 3D dosimeter is undergoing treatment, a motion is simulated much like a tumour would be within a patient [1]. Once the treatment is finished, the 3D dosimeter is removed and scanned using a dual wave-length optical scanner. The motion to the tumour may be simulated by use of a Hexamotion system available at the RNSH [1]. A diagram of the set up may be seen in figure 2.2.

There have been new developments into introducing tracking devices to radiotherapy centres. The RNSH has been fitted with an electromagnetic tracking device, where the

detected motion is fed back to the linear accelerator utilising a DMLC. This allows more precise radiation to hit the tumour, sparing the healthy tissue.

Ceberg (2010) discussed a DMLC with tumour tracking, which adjusts the radiation beam according to the motion of the tumour. It also continuously aligns itself, while reshaping the machine aperture to follow the tumour. This is called the DMLC real time tumour tracking system, designed at Stanford University [11]. A breathing simulation equipment in radiotherapy (BERT) robot was also designed to simulate the movement of lungs. This corresponded to the inspiration and expiration breathing phases. This allows a tighter margin around a tumour by constantly changing the radiation beams according to the motion of the tumour. With this technique, a higher radiation dose may be given.

The DMLC will also switch off the radiation beam if the patient experiences movement, such as coughing [11]. However, there are some uncertainties associated with the tracking system. Such as any delay between the tumour moving and the DMLC repositioning the radiation beam, and any differences in the output due to the use of motion tracking instead of a static model. To identify if there is any dose rate variation that may be caused from the motion of the tumour, the dose rate profile should be compared to that of a static model. This is also a limiting factor.

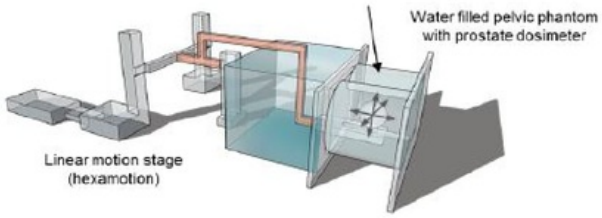

Figure 2.2: *The prostate tumour radiation dosimeter is mounted on to the Hexamotion platform within the pelvic phantom. The pelvic phantom is filled with water to simulate human tissue. Radiation is delivered to the dosimeter, while the Hexamotion mimics physiological movement a prostate tumour would make when in a patient. [1]*

2.6 Accuracy

Not only have both polymer and elastomer gel dosimeters been applicable in measuring radiation doses in 2D, but they have now been able to verify the radiation dose distribution in three dimensions. The issue is, to what degree of accuracy? For 3D dosimeters to be implemented in the medical industry, a clinically acceptable uncertainty must be met. [13]

A problem that arises when analysing the dose distribution is with the standards to which the irradiated dosimeter should be compared upon. At the present moment, the dose distribution on the irradiated dosimeter are compared with another dose distribution which used a reliable dosimetry technique. An example would be a single photon or electric field compared with an ionisation chamber or diamond detector [3]. There are a number of factors that do affect accuracy, though not all are discussed in this study. These include:

- Temperature during curing, radiation, and imaging
- Tissue equivalence
- Discrepancies between the calibration vial and dosimeter in fabrication
- Positioning error of calibration dosimeter
- Chemical instabilities
- Recipient wall effects
- Dose rate and energy dependent response
- Artefact in imaging
- Voxel shape (bandwidth)
- Spatial inaccuracy
[3, 11, 19]

Chapter 3

Methods and Materials

3.1 Fabrication

The FlexyDos3D dosimeter is relatively simple to fabricate as it consists of only a few components. The elastomer gel contains the PDMS elastomer (SYLGARD® 184), with only a small percentage being the initiator chloroform ($CHCl_3$) and the radiation sensitive additive LMG. In the effect of initiators on the stability experiment (section 4.1), the properties of FlexyDos3D are studied when chloroform is replaced with dibromomethane (CH_2Br_2) as the initiator. The concentrations of the different components are crucial when manufacturing FlexyDos3D, and thus remain the same unless specified otherwise. De Deene (2015) goes further into detail with the optimal concentrations for a responsive FlexyDos3D elastomer gel [13]. In Hanif (2016) the chemical concentrations within FlexyDos3D was taken at 90% SYLGARD® 184, 7% SYLGARD® curing agent, 3% $CHCl_3$, and 0.03% LMG [12]. This composition is referred to as the nominal concentrations.

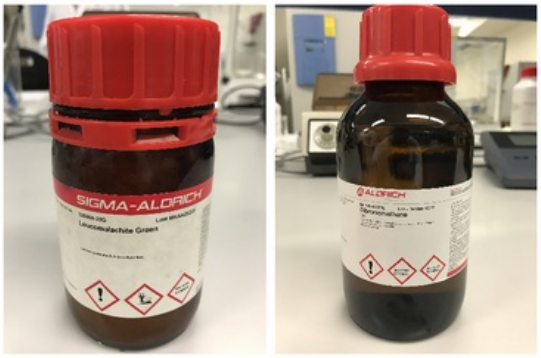

Figure 3.1: *Both the LMG (left side) and dibromomethane (right side) were acquired from Sigma Aldrich Australia.*

SYLGARD® 184 and the SYLGARD® curing agent were measured using a scale accurate to 0.01g, while the remaining components such as chloroform, dibromomethane

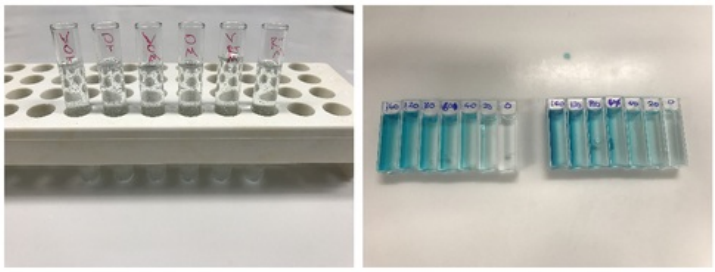

Figure 3.2: *Left image shows the glass test tube samples (non-irradiated). Right image shows the cuvette samples after irradiation at various times.*

and LMG on a scale accurate to 0.00001g. It was also crucial to have clean beakers and utensils as not to contaminate the FlexyDos3D elastomer gel. To decrease the likelihood of contamination, all the beakers and utensils were rinsed with deionised water, and dried in the oven.

The fabrication procedure begins with the components being weighed within their own respective beakers, avoiding any reaction that might occur before the components are combined. The SYLGARD® 184 and curing agent were placed into one beaker, while the chloroform or dibromomethane with LMG in another. Only upon all the components being accurately weighed were they combined. Chloroform was added immediately to the components given its highly volatile properties. The combined components were stirred well to ensure uniformity throughout the elastomer gel.

The FlexyDos3D elastomer gel was poured into the desired number of polymethyl methacrylate (PMMA) cuvettes, glass test tubes, or moulds. The weight within the cuvettes is not critical, so long as the elastomer gel covers the field of view for the spectrophotometer when reading the optical density (OD) as mentioned in section 3.3. The weights within the glass test tubes are kept at 2.5 grams throughout.

The stirring of the elastomer gel creates air bubbles within. This is not a desired effect, as the elastomer gel, when cured, will result in scanning artefacts. To remove the air bubbles, the elastomer gel within the cuvettes, test tubes, or container are placed into a vacuum desiccator. In some of the experiments within this study, the method does not require the vacuum desiccator to be used as per the investigation parameters. To remove all the air bubbles within the elastomer gel, vacuum pumping was performed above the samples, several times, until all air bubbles were removed. Vacuum pumping was done on the entire batch, unless where specified otherwise for certain individual samples.

After the removal of the air bubbles in the vacuum desiccator, the FlexyDos3D elastomer gel samples were cured. This involved heating in an oven at 60^oC for a specified time, or allowed to cure at room temperatures. Those at room temperatures were placed in a dark cabinet away from any light, to avoid the FlexyDos3D elastomer gel responding to UV radiation. The elastomer gel requires 48 hours to fully cure at room temperatures. Some experimental methods involved curing the samples using both the oven and then

room temperatures.

If samples were cured using an oven, they were allowed to sit in a dark cabinet away from any light for a duration of 30 minutes, to bring these samples to room temperatures, before irradiation.

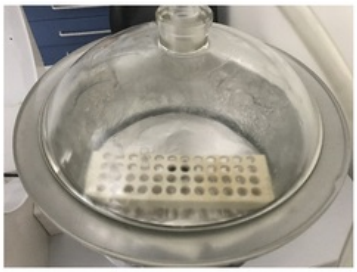

Figure 3.3: *The vacuum desiccator used for removing air bubbles within samples. A vacuum was required to be pulled several times before all air bubbles were removed.*

Figure 3.4: *The oven used for curing samples throughout this study.*

3.2 Irradiation

The elastomer samples were then irradiated with UV radiation. This was achieved by placing the sample at a distance of 80mm away from the UV radiation source. For the cuvettes to be read out with the spectrophotometer, they are only required to be irradiated on one side. In the case of the test tubes, they were rotated to achieve a uniform exposure to the UV radiation. This was done by attaching the test tube to a mechanical rotator, as seen in figure 3.5. The orientation of the test tubes varied when irradiating and scanning, and is mentioned in section 4.2.

To prevent any UV radiation exposure to personnel in the laboratory, the UV radiation source was covered. When irradiating the cuvettes, a small wooden cover was used. When irradiating the test tubes, a large cardboard box was used. This was necessary due to the size of the set up (mechanical rotator and UV radiation source). The irradiation time is dependent on the experimental method.

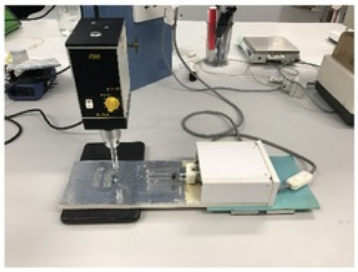

Figure 3.5: *This apparatus consists of a mechanical rotator (left side), UV radiation source (right side), and is used to irradiate test tube samples. The apparatus is covered by a box to avoid UV radiation exposure to personnel.*

3.3 Scanning

For the study of the radiation properties, a spectrophotometer (USB4000, ocean optics) was used. For the spatial characterisation of the dosimeters, an optical scanner constructed by the Macquarie University research group was used. With both procedures, the lights in the room were switched off when the samples were outside of the contained environment.

The spectrophotometer returns the OD relevant to the wavelength chosen. The two chosen wavelengths used were 630nm and 400nm. These correspond with the study by Hanif (2016) and De Deene (2015) [1, 12]. Before measuring the cuvette samples, a reference cuvette sample containing deionised water was used in the spectrophotometer. Deionised water was an acceptable reference standard as shown by De Deene (2015), comparable to FlexyDos3D without the LMG [13]. This was done for both the 400nm and 630nm wavelengths. The measured OD for each individual sample is seen in equation 3.1.

$$\Delta OD = OD_{(630nm)} - OD_{(400nm)} \tag{3.1}$$

The test tube samples required the FlexyDos3D to be removed from the glass prior to being placed in the optical scanner, to avoid light refraction. This was done by breaking the glass. The FlexyDos3D also required a rinse in water to remove any small fragments. A holder for the test tube samples within the optical scanner was fabricated prior to this study, and made from a silicon elastomer. The orientation of the test tube samples in the holder, were dependent on the method used in the experiments. The sample also had to be as perpendicular to the holder as possible. If the sample were to be slightly slanted, it would have created larger room for errors when reconstructing. For the samples to be scanned on the day of fabrication, they were scanned in the optical scanner holder in a single reading. The optical scanner was then initialised using scripts in MATLAB, and the resulting images were used for reconstruction. Here the two light sources were red and blue [1].

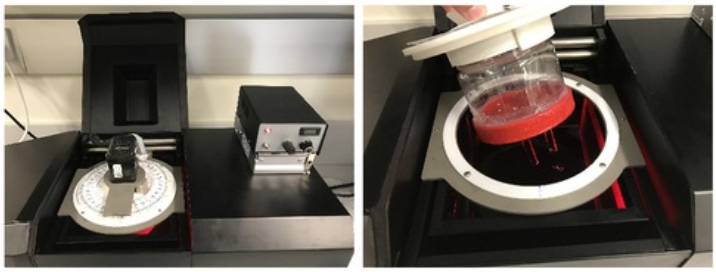

Figure 3.6: *The optical scanner used at Macquarie University. The left image shows the stepper motor used to rotate the samples* 360^o*, along with the switch to change the light source from blue to red. The right image displays the holder, which sits in a vat of glycerol fluid.*

The cuvette samples did not require any reconstruction. The regions of interest for the test tube samples were the most responsive regions. In figure 3.7 they can be seen with a rectangle box around.

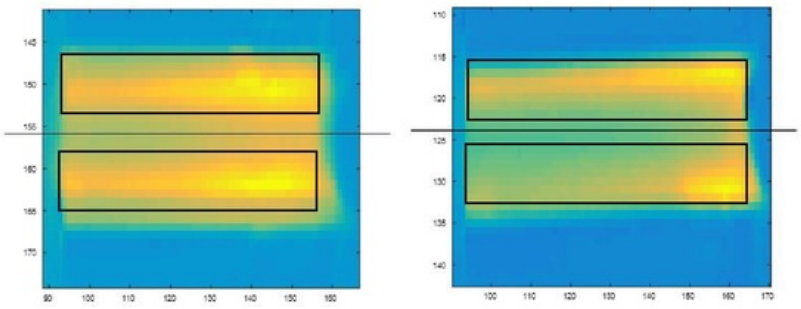

Figure 3.7: *Both images are cross sections of the test tube samples. The colour corresponds to the OD (i.e. yellow is high OD, blue is low OD). The regions of interest are the most responsive regions (yellow), situated on the outer edge of the samples. The UV radiation could not penetrate across the whole cross section of the samples. The rectangle sizes are consistent for all images.*

To obtain the OD from the regions of interest, a script was written in MATLAB. The script worked by selecting a rectangle of a certain size over the regions of interest as seen in figure 3.7. The script then returned the average OD for each column of pixels, of both upper and bottom rectangles, and plotted it against the distance (in pixels).

3.4 Storage

Previous studies have shown that the storing temperatures are a factor on the stability of the OD in FlexyDos3D. Hanif (2016) goes into detail about the most suitable temperatures. For consistency, the three storing temperatures used were the same as in Hanif (2016). These were: room temperatures (20^oC), fridge (4^oC), and freezer (-81^oC) [12]. Each experimental method specifies the duration the samples were to be stored in these temperatures. It is important the samples have minimal exposure to light, as to not increase the OD and give room for larger errors in the readings.

Chapter 4

Experimental Procedures

4.1 The Effect of Initiators on the Stability

Chloroform is currently used within FlexyDos3D as a radical initiator. De Deene (2015) talks about the use of chloroform within FlexyDos3D in more detail [13]. A significant issue with the stability of FlexyDos3D remains when chloroform is used as the initiator within. Post manufacturing, the stability slowly degrades over time. It also is dependent on the storage temperature as investigated in Hanif (2016) [12]. To date there have been no successful solutions eliminating the degrading stability entirely. It has, however, been found that if FlexyDos3D is stored in cold temperatures, the degrading stability is slowed significantly. It has then been suggested to search for an alternate initiator for the FlexyDos3D elastomer gel that may behave in a more suitable way than chloroform. Further research into replacing the chloroform with other initiators to investigate the effect of radicals on the dose response, stability, and dose-rate dependency was done in Hoye et al (2015) [9]. Recently, the molecular structure of dibromomethane has been investigated, and is suspected to behave in a similar manner to chloroform yet potentially may be more suitable for the intended use of FlexyDos3D. This experiment was then to investigate the feasibility of using dibromomethane over chloroform within FelxyDos3D.

The FlexyDos3D elastomer gel with dibromomethane were manufactured using the same method as specified in the previous fabrication section 3.1. Two batches were fabricated, using either chloroform or dibromomethane as initiators. All the concentrations of the components remained the same, and both the chloroform and dibromomethane concentrations were identical. Table 4.1 shows the nominal concentrations and weights. Both batches were placed within a desiccator to remove any bubbles within the elastomer gel, and then into the oven to be cured for 60 minutes at 60^oC. Upon curing, the cuvettes were left in a dark cabinet to return back to room temperatures before being exposed to UV radiation.

Both the chloroform and dibromomethane cuvettes were divided into three groups of seven. Each group of cuvettes were exposed to UV radiation for 0s, 20s, 40s, 60s, 80s, 120s, and 160s. After the FlexyDos3D elastomer gel was exposed to UV radiation, the OD was recorded using the spectrophotometer. The OD of each cuvette was measured

Table 4.1: The weights and nominal concentrations used for both chloroform and dibromomethane batches in FlexyDos3D

	SYLGARD® 184 (90%)	SYLGARD® Curing Agent (7%)	$CHCl_3$ or CH_2Br_2 (3%)	LMG (0.03%)	Total Weight	No. of Cuvettes
$CHCl_3$	72g	5.6g	2.4g	0.024g	80g	21
CH_2Br_2	104.4g	8.1g	3.48g	0.034g	116g	30

at both 400nm and 630 nm wavelengths, where a cuvette filled with deionised water was used as a reference for both these wavelengths and all following readings. The results gathered right after exposure were marked as day zero.

The samples were then stored at three separate temperatures. These were: room temperatures (20^oC), fridge (4^oC), and freezer (-81^oC). These temperatures were also used in Hanifs (2016) study [12]. After 24 hrs, the cuvette samples were removed from their respective storages, and allowed to sit in a dark cabinet for 30 min to return to room temperatures before the OD was read once again. At 30 min, the OD of the samples were read with the spectrophotometer. This was repeated for all samples every 24 hrs, over a four-day period. The results were plotted to see the overall responses with respect to the temperatures and durations the samples were stored at.

Nine samples remaining from the dibromomethane batch were exposed to UV radiation for 40 s, after fabrication, to determine the measurement precision of the spectrophotometer. The measured error was applied to every reading for both the chloroform and dibromomethane batches.

4.2 Investigating Potential Chloroform Evaporation

In Hanif (2016), it was observed that the OD was higher near the edges of the sample, suggesting a higher responsiveness of the dosimeter near the edges [12]. This increase in OD around the edges did not occur when the elastomer gel is irradiated immediately after fabrication and when the elastomer gel was scanned immediately after irradiation. A possible explanation is that the chloroform initiator is evaporating, which occurs faster at the edges of the phantom, leading to a heterogeneous in the phantom. In the previous experiment 4.1 on the effect of initiators on the stability, it was observed that the stability increased with colder storage temperatures. It is assumed that decreased temperatures slow down the auto-oxidation reactions, allowing the dosimeter to be more stable. This was also observed in Hanif (2016) [12].

This experiment investigates the potential evaporation of chloroform by exposing FlexyDos3D samples to various curing procedures and temperatures. The FlexyDos3D mixture was poured in glass test tubes. The samples were exposed to UV radiation and scanned with the optical scanner for specified times. The potential chloroform evaporation was investigated through two experiments. For both experiments, the same method was followed, with the only difference being the position of the samples during irradiation and scanning. The first experiment involved having the samples in an upright position

(open end of the test tube on top), while the second involved the samples in a downright position (open end of the test tube facing down).

If the resulting OD profile along the direction of exposure would exhibit a similar heterogeneity in both experiments, regardless the orientation of the sample, it could be concluded that the UV radiation source was causing the non-uniformity. If the profile however displayed an opposite trend (i.e. the non-uniformity depends on the direction in which the sample was positioned with respect to the lamp), it can be concluded that the heterogeneity in OD was attributed to chemical processes within the sample.

All the FlexyDos3D samples were manufactured using the standard procedure as mention in section 3.1. However, each sample was cured and stored differently. The nominal concentrations of the components were used as seen in table 4.2, along with the weights. Each test tube contained 2.5 grams of FlexyDos3D.

Table 4.2: The weights and nominal concentrations used for the upright and downright position experiments

	SYLGARD® 184 (90%)	SYLGARD® Curing Agent (7%)	$CHCl_3$ (3%)	LMG (0.03%)	Total Weight	No. of Test Tubes
Upright Position	27g	2.1g	0.9g	0.009g	30g	10
Downright Position	36g	2.8g	1.2g	0.012g	40g	15

Table 4.3 displays the various curing procedures and temperatures the samples underwent. Some samples did not undergo a vacuum treatment in the vacuum desiccator, which resulted in some air bubbles remaining present when cured. The air bubbles are clearly visible in the images, as slightly increased OD.

All the samples were irradiated for a duration of 5 minutes on the same day of the scan. This was completed by utilising the mechanical rotator apparatus, as shown in figure 3.5. This guaranteed a uniform angular exposure to UV radiation. Further detail is mentioned in section 3.2.

The resulting OD profile in figures 5.4 and 5.5, show the positioning of the test tubes when being exposed to the UV radiation. The mechanical rotator grips the upright position experiment test tubes upside down (open end of the test tube on the bottom), while the downright position experiment are gripped at the open end. If any chloroform were to evaporate, it would evaporate from the open end of the test tube. This particular region was of interest to the experiment.

After irradiation, the dosimeters were removed from the test tubes. The scanning procedure followed the same method as aforementioned in 3.3.

Table 4.3: The various curing procedures used for the upright and downright position experiments. The "x" indicates the sample underwent this method.

Sample Name	Desiccator	Oven	Scanned On Day of Fabrication	Scanned 72Hrs After Fabrication
RT-72HrsPostFab	-	-	-	x
Vac-RT-72HrsPostFab	x	-	-	x
Oven-RT-72HrsPostFab	-	x	-	x
Vac-Oven-RT-72HrsPostFab	x	x	-	x
Oven-OnDay	-	x	x	-
Vac-Oven-Onday	x	x	x	-

4.3 Dependence of the Stability on Curing Agent

In the experiment where the effect of different initiators were studies, the results displayed improved chloroform stability at room temperatures. This improved stability has not been found in previous studies. Though the stability of chloroform at room temperatures over time is still not desirable for use, the improved stability shown in the Dibromomethane and Chloroform Experiment led to the conclusion of inadvertently finding optimal concentrations for FlexyDos3D. Presently there have been no studies that investigate the ideal concentration of the curing agent in FlexyDos3D. De Deene (2015) studied the concentrations of chloroform and LMG within FlexyDos3D, though the curing agent has not been studied.

This experiment investigates various concentrations of the SYLGARD® Curing Agent, and its effect on the stability of FlexyDos3D. These concentrations are shown in table 4.4 and vary from 1-15%.

The FlexyDos3D elastomer gel was manufactured using the standard procedure mentioned in 3.1. The only variation made in this method was the concentration of curing agent. This experiment originally commenced with concentrations of 5-15%. These results werent beneficial to the stability of FlexyDos3D, and hence the experiment further investigated the use of concentrations from 1-4.5%.

The FlexyDos3D elastomer gel was poured into a number of cuvettes, to be irradiated for 0, 20, 40, 80, 120, and 160s. The cuvettes were then scanned using the standard scanning procedure for the spectrophotometer mentioned in section 3.3. That is, a cuvette filled with deionised water was used as a reference for both 400nm and 630nm wavelengths on the spectrophotometer. After exposure and the OD readings, the cuvettes were stored in a dark cabinet at room temperatures. The OD was gathered over a duration of three days.

Table 4.4: The various batches concentrations and weights, for curing agent concentrations 1-15%.

SYLGARD® Curing Agent		SYLGARD® 184		$CHCl_3$		LMG	
Conc. (%)	Mass (g)	Conc. (%)	Mass (g)	Conc. (%)	Mass (g)	Conc. (%)	Mass (g)
1%	0.25	96%	24	3%	0.75	0.03%	0.0075
2%	0.5	95%	23.75	3%	0.75	0.03%	0.0075
3%	0.75	94%	23.5	3%	0.75	0.03%	0.0075
4%	1	93%	23.25	3%	0.75	0.03%	0.0075
4.5%	1.125	92.5%	23.125	3%	0.75	0.03%	0.0075
5%	1.25	92%	23	3%	0.75	0.03%	0.0075
7.5%	1.875	89.5%	22.375	3%	0.75	0.03%	0.0075
10%	2.5	87%	21.75	3%	0.75	0.03%	0.0075
12.5%	3.125	84.5%	21.125	3%	0.75	0.03%	0.0075
15%	3.75	82%	20.5	3%	0.75	0.03%	0.0075

4.4 3D Printing of Prostate Phantom

To apply the findings found in this study to a more real world application, a prostate tumour model was designed and fabricated. The model was a mould, in which the FlexyDos3D elastomer gel can be poured within. The resulting product is a three dimensional FlexyDos3D dosimeter. This radiation sensitive prostate tumour dosimeter may be used for radiotherapy dose verification, involving the dosimeter undergoing the same radiation treatment a patient would undergo, in hope to improve the quality assurance procedure of IMGRT. However, this study did not involve any 3D dosimeters undergoing exposure to high-energetic x-rays. Rather, the experiment in particular is the final step in preparation for placing a 3D radiation dosimeter through a radiation treatment plan.

The mould was designed to be 3D printed for convenience, and also serve as the housing for the 3D radiation dosimeter when being irradiated. Previously there have been issues with positioning the dosimeter in the exact same location when irradiating. Having the mould as the housing ensures the dosimeter sits in the exact position at all times when irradiating, even if there is repositioning. The mould itself is mounted to the platform of the Hexamotion, seen in figure 3.5, by several bolts. The Hexamotion will be simulating movements the tumour would make whilst in a patient. The radiation dosimeter may be removed by breaking the 3D printed mould.

The experiment involved utilising an already rendered 3D model of a prostate tumour, and edited using Autodesk Meshmixer. The steps taken in editing the prostate tumour model are as below.

1. Removed attached organs to acquire only the prostate tumour.
2. Performed a boolean difference of 4mm, creating a cavity within the prostate tumour for the FlexyDos3D elastomer gel to be poured in.
3. Attached a cube to the front of the tumour, which goes into the cavity. This leaves

a cube shaped hole in the dosimeter, which will be used for mounting the dosimeter on to the optical scanner.

4. Removed material from the topside of the mould, leaving an opening for the Flexy-Dos3D elastomer gel to be poured through

5. Created a baseplate on which the prostate tumour mould will be attached to. This baseplate will be used for mounting the mould to the platform of the Hexamotion.

The prostate tumour mould was printed using a FlashForge Dreamer 3D Printer. This was out of the materials Acrylonitrile-Butadiene-Styrene (ABS) or Polylactic Acid (PLA), with a soluble filament as the support structure. Since the mould itself will be housing the dosimeter suspended in a pelvic phantom filled with water, when undergoing radiation, the electron density of the materials were checked to ensure they are close to that of water. They were 1.01 and 1.14 respectively [20,21]. Both these electron densities are considered reasonable, and are not expected to change the response of the radiation dosimeter upon irradiation. All the filaments used were trial printed using the manufacturers specified temperatures for the nozzle and platform. Later these temperatures were adjusted, but never more or less than 20^oC from the manufacturers specified temperatures.

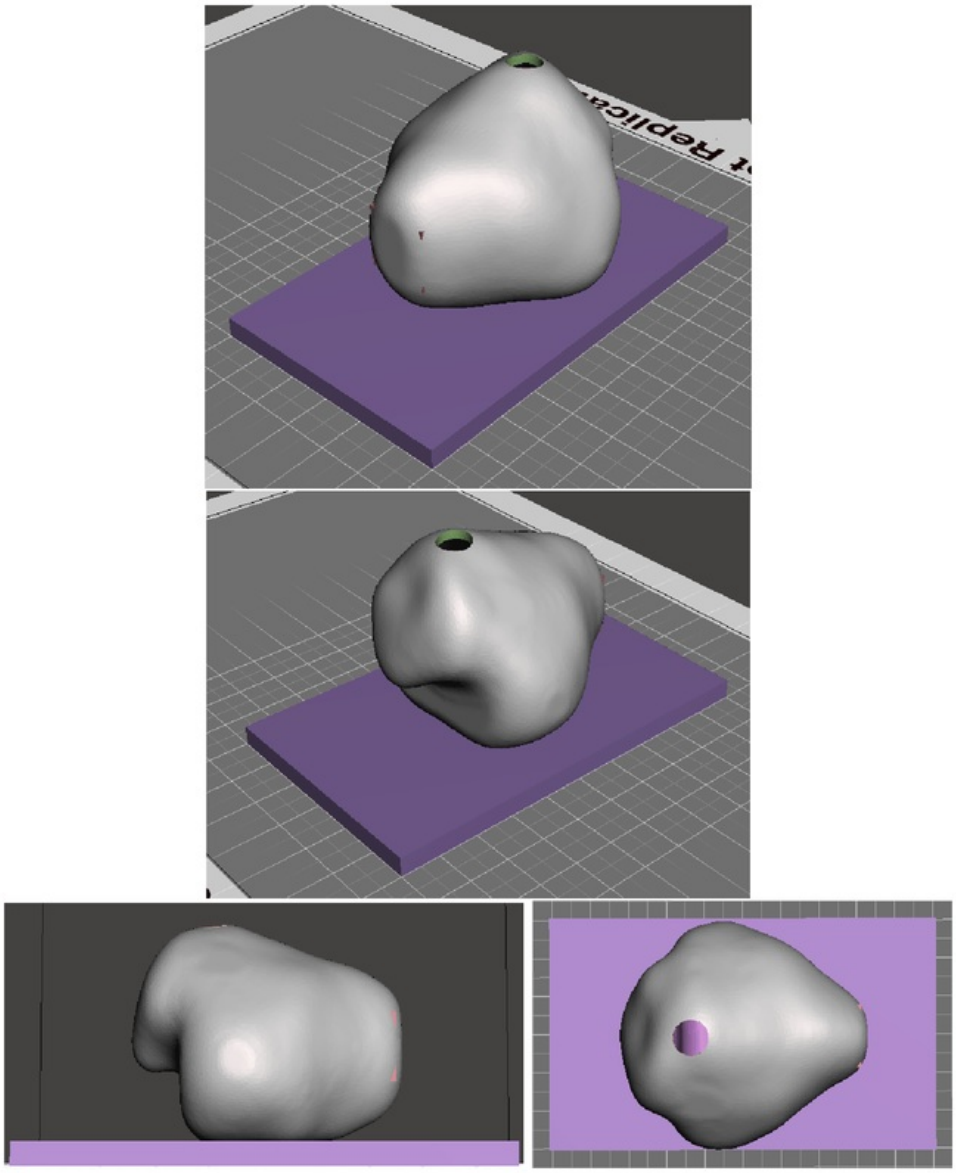

Figure 4.1: *The 3D prostate tumour mould rendered in the Meshmixer mixer software, along with all the modifications*

4.5 Mechanical Properties

With the conclusion to utilise 4-4.5% curing agent concnetration in section 5.3, being able to identify the mechanical properties would prove to be beneficial for using FlexyDos3D in other applications. The SYLGARD® 184 Safety Data Sheet (SDS) specified the tensile strength, but at the recommended 10% curing agent concentration [22]. However, using FlexyDos3D at 4-4.5% is more desirable for future studies of radiation dosimeters.

To determine its mechanical properties, several specimens were manufactured to undergo tensile testing. To produce these specimens, new moulds were designed and fabricated using the FlashForge Dreamer 3D printer. The tensile testing specimens were fabricated in accordance with Australian Standards. In this experiment, the mechanical properties of 4%, 4.5%, and 5% curing agent concentration were investigated and compared. The properties of interest were found from the stress on strain graph seen in figure 5.9, showing the Ultimate Tensile Strength (UTS) and Youngs Modulus.

The tensile testing moulds were designed using Creo Parametric 2.0. The mould can be seen in figure 4.2, and was printed using the PLA material on the FlashForge Dreamer 3D printer.

The FlexyDos3D elastomer gel was manufactured using the standard procedure mentioned in section 3.1. The only variance to the procedure was the curing agent concentration. When using low curing agent concentrations, the elastomer was relatively soft and tacky. To avoid the elastomer sticking to the mould, petroleum jelly was rubbed onto the mould. Petroleum jelly is used in many applications for releasing elastomer's from other materials. It is unsure whether or not petroleum jelly does react with any of the components within FlexyDos3D, Further investigations should be conducted. The elastomer was then placed into the desiccator to remove any air bubbles, and then into the oven at 60^oC for two hours.

The tensile test could not be performed on the Instron Mechanical Testing System at Macquarie University. This system was designed for metals. If the tests were done on the Instron, there would be no method of determining the accuracy of the readings. The tensile tests had to then be done manually. This was by clamping the specimens to a retort stand, and slowly adding mass on the bottom of the specimens. Water was used as the weight, and added in increments of 5 ml, until failure. The change in length was measured every increment. The data gathered was plotted as a stress on strain graph.

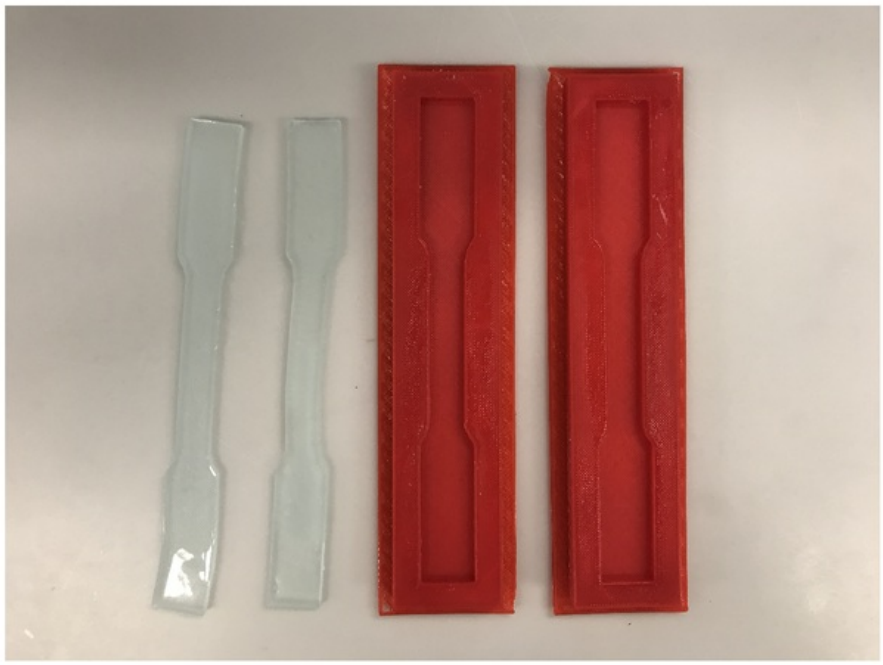

Figure 4.2: *Two tensile testing moulds were fabricated from PLA using the Flashforge Dreamer 3D printer. The tensile testing specimens fabricated from FlexyDos3D can be seen on the left.*

Chapter 5

Results and Evaluation

5.1 The Effect of Initiators on the Stability

The consistent drop in OD for chloroform over time left at room temperatures as seen in figure 5.1(b), was not similar to the results gathered in Hanif (2016), even though the same concentrations were used [12]. Neither was it similar to the interpolated results in De Deene (2015) [13]. A possible explanation may be with the component concentrations within the FlexyDos3D elastomer gel. The error in the concentrations may have been larger than thought. The graph for OD versus Dose for Chloroform was not as expected as it resulted in a more stable response over time, than found in both De Deene (2015) and Hanif (2016) [12, 13]. This study produced a FlexyDos3D elastomer that was more optimal than compared with previous studies, despite the concentrations being the same as those used by De Deene and Hanif.

Figure 5.1(a) showing the graph displaying the OD versus radiation exposure for different dibromomethane samples, behaves much like that of chloroform in Hanif (2016) and De Deene (2015) [12, 13]. It was not evident that using dibromomethane over chloroform at room temperatures was more suitable. Rather, using dibromomethane provides similar characteristics and stability as chloroform at room temperatures after irradiation.

Figure 5.2(b) showing the graph displaying the OD versus radiation exposure for different chloroform samples at fridge temperatures, behaves in a more stable manner than that stored at room temperatures. The gradients of the trendlines over the four days are very close to one another. However, there was an offset between each day. This behaviour is similar to that of Hanif (2016), though the offsets here are smaller [12]. This may be due to the possible find of an optimal concentration for FlexyDos3D, as mentioned earlier.

The graph shown in figure 5.2(a) depicting the dibromomethane in FlexyDos3D at fridge temperatures, displays a more stable response when stored at fridge temperatures compared to room temperatures. However, it is evident when comparing the stability between both dibromomethane and chloroform at fridge temperatures, that dibromomethane is less suitable.

When using either the chloroform or dibromomethane, as the initiator in FlexyDos3D,

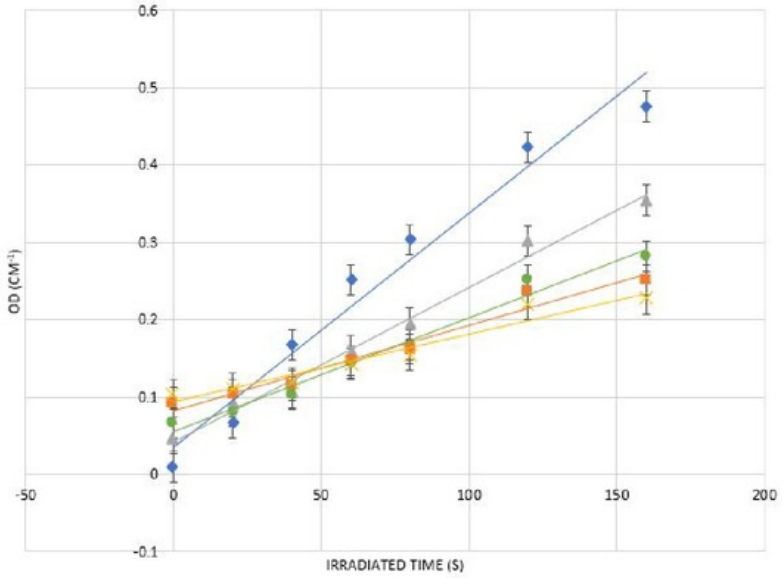

(a)

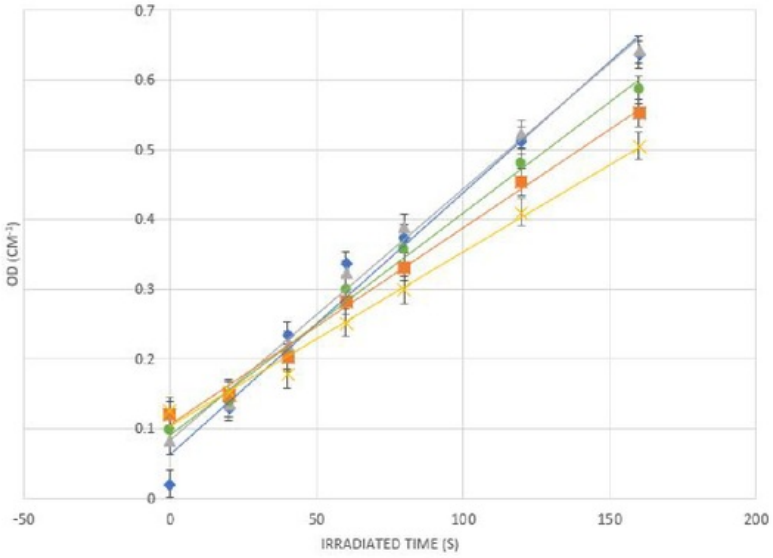

(b)

Figure 5.1: *Both graphs display the resulting change in OD at room temperatures when using the dibromomethane (a), and chloroform (b) initiators within Flexydos3D. This was over several irradiation times, on day 0 (blue), day 1 (grey), day 2 (green), day 3 (orange), and day 4 (yellow). A linear trendline was fitted across the different irradiated times of each day. The chloroform can be seen to be more stable, and subsequently a more suitable initiator within FlexyDos3D.*

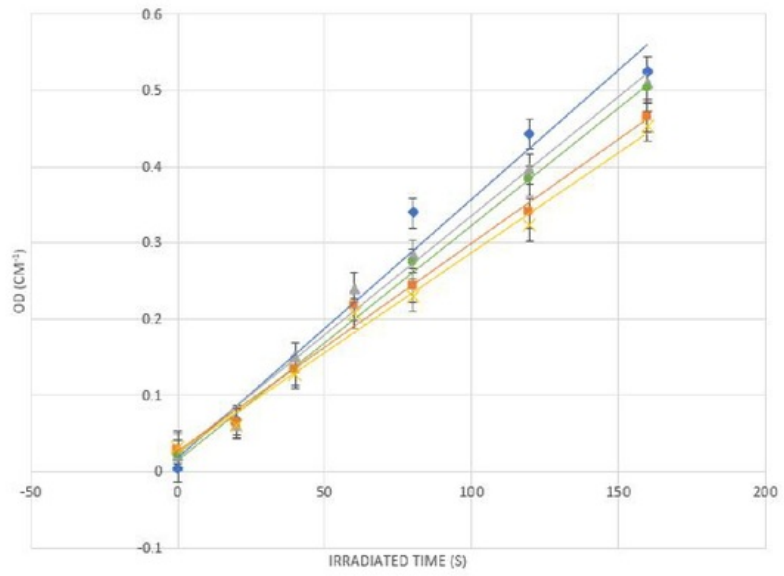

(a)

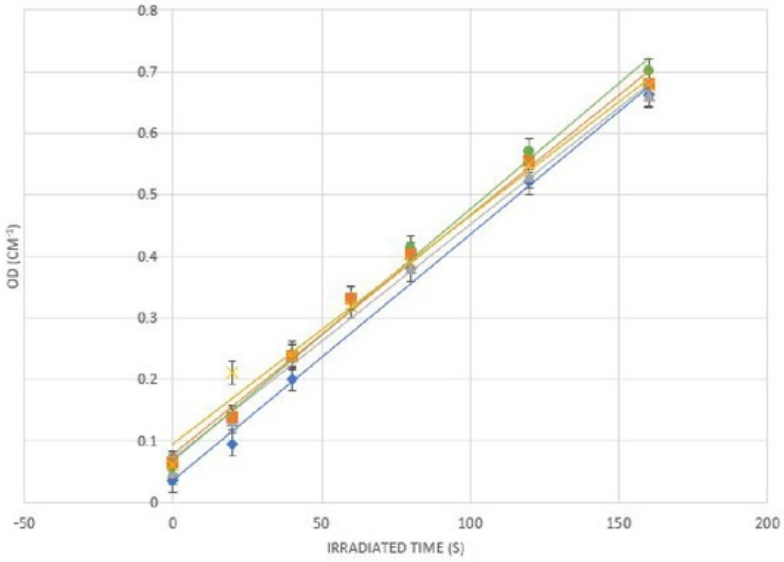

(b)

Figure 5.2: *Both graphs display the resulting change in OD at fridge temperatures when using the dibromomethane (a), and chloroform (b) initiators within Flexydos3D. This was over several irradiation times, on day 0 (blue), day 1 (grey), day 2 (green), day 3 (orange), and day 4 (yellow). A linear trendline was fitted across the different irradiated times of each day. The chloroform can be seen to be more stable, and subsequently a more suitable initiator within FlexyDos3D.*

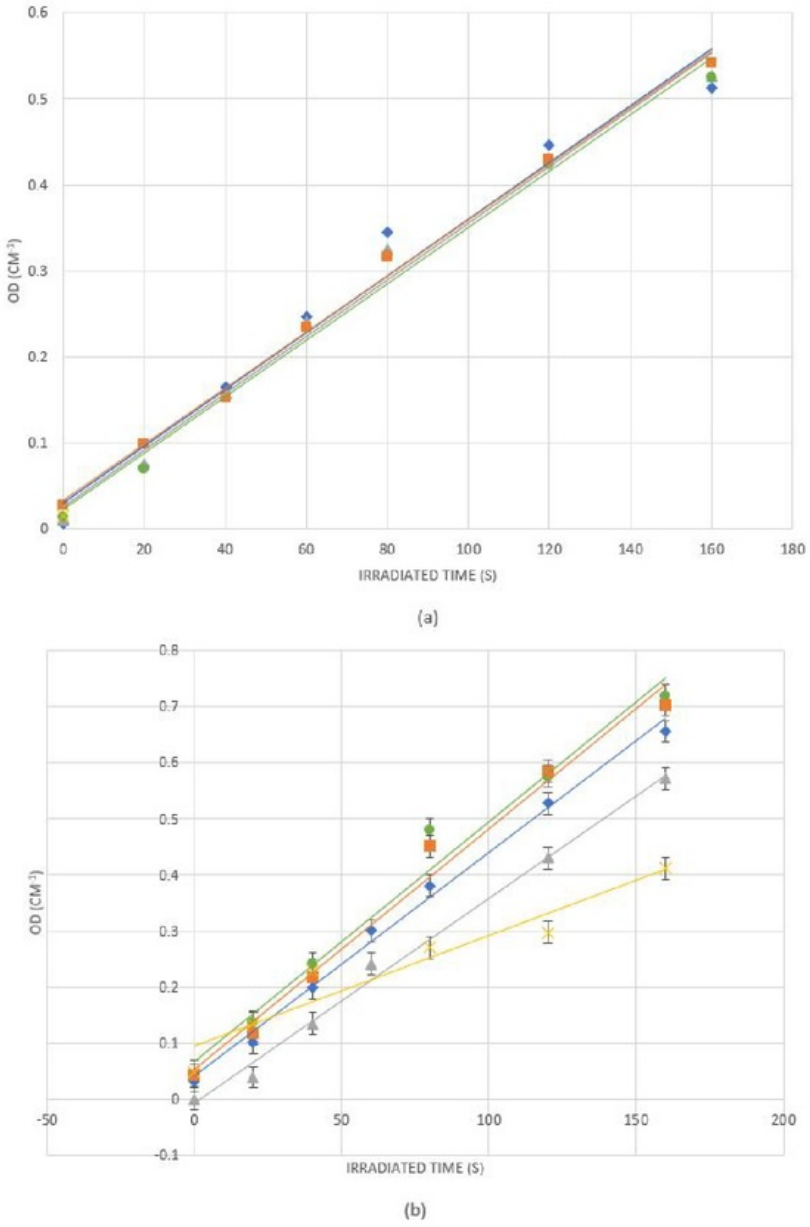

Figure 5.3: *Both graphs display the resulting change in OD at freezer temperatures when using the dibromomethane (a), and chloroform (b) initiators within Flexydos3D. This was over several irradiation times, on day 0 (blue), day 1 (grey), day 2 (green), day 3 (orange), and day 4 (yellow). A linear trendline was fitted across the different irradiated times of each day. The dibromomethane can be seen to be more stable at freezer temperatures.*

proved to be most stable when stored in the freezer, as seen in figure 5.3. Chloroform at freezer temperatures in figure 5.3(b), shows a similar trend as that shown in the fridge. The gradients of each trendline of chloroform in the freezer are similar for the duration over 4 days, but there remains an offset between each. This offset seems to be increasing the longer the chloroform samples are stored in the freezer. However, these offsets do not indicate that the OD is only dropping over time, but rather either increases or decreases over time. This is the same as the chloroform graph when stored in the fridge, but not when stored at room temperatures. The results for the measurements performed four days after exposure are shown to be very irregular, with the gradient dropping dramatically. This has not been observed with any other temperature, or in Hanif (2016) [12]. The reason remains unknown.

The dibromomethane graph for storage at freezer temperatures, as seen in figure 5.3(a), seems to be very promising. There is no difference in the gradient of the trendlines for each day, and the offset is so minute that it's negligible. The stability of FlexyDos3D at freezer temperatures when using dibromomethane was ideal, and proved to be a suitable method for retaining the original OD several days after being irradiated.

When comparing the use of dibromomethane and chloroform as the initiator in FlexyDos3D, chloroform is found to be most suitable when stored in either the fridge or room temperatures. Dibromomethane is found to be most suitable for storage in the freezer. However, it was noted that the stability of chloroform was significantly better than in previous studies. A plausible explanation is attributed to the differences in FlexyDos3D composition. Another study is needed to investigate the concentrations within FlexyDos3D, specifically the SYLGARD® curing agent, which has not been previously studied. It can be concluded that chloroform in FlexyDos3D is a more stable and suitable initiator than dibromomethane in fridge and room temperatures. Dibromomethane is more stable at freeze temperatures compared to chloroform at freezer temperatures, though the use of such a low temperature is not practical.

5.2 Investigating Potential Chloroform Evaporation

Figure 5.4 depicts the change in OD over the length of the sample in the upright position, showing a gradual increase of OD from the bottom of the sample to the top (open end). The overall profiles of the downright position samples in figure 5.5 are different to that seen in the upright position (figure 5.4). Here the profile is flat throughout, with a small increase in OD at the end of the samples. To prove that the heterogeneity in OD is true (i.e. attributed to non-uniformity of the UV radiation source or chemical processes within the samples), the profiles of the downright position samples would be required to be similar to that of the upright position. That is, the resulting OD profile increases along the direction of exposure, or the OD profile results in a opposite trend. This, however, is not the case, indicating these scenarios are not true.

A possible scenario for the behaviour of the resulting OD profiles in both the upright and downright position experiments, may be due to reconstruction errors. To check if

this scenario is true, two tests were conducted. This was performed by scanning several FlexyDos3D samples that had completely responded to the UV radiation (i.e. were irradiated for an extensive period of time). One sample, had its chloroform and LMG irradiated prior to the components being combined in the fabrication procedure. The other, was a sample irradiated after fabrication and curing. Both resulting graphs for the OD over time, were a horizontal line, indicating there was no change in OD (as expected). Henceforth, no errors in the reconstruction of the images. Appendix A shows the graphs for both irradiated samples. This eliminates the scenario of reconstruction errors being the cause for the resulting OD profiles shown for the upright and downright position experiments.

The slight increase in OD at the end of the downright samples (figure 5.5) is due to the concave shaped glass at the bottom of the test tube. This causes the UV radiation to converge at that region, subsequently raising the OD at the end of the sample. The shapes of the sample profiles are almost identical to one another, with only noise varying throughout.

The upright position samples resulting OD profiles, seen in figure 5.4, shows that the various curing procedures are similar, and do not deviate far from one another. The samples that were irradiated and scanned on the day of fabrication, had a higher peak in OD when compared to the remaining samples. This was not evident in the resulting OD profile of the downright position seen in figure 5.5. The downright position samples which were irradiated on the same day as fabrication, had a far lower OD response than those irradiated 72hrs after. It is also seen that curing samples by the use of an oven, and allowing it to sit at room temperature for 72hrs, raised the OD higher than that of any other sample. However, there is no correlation between the OD in either setting for samples with or without being in a vacuum desiccator.

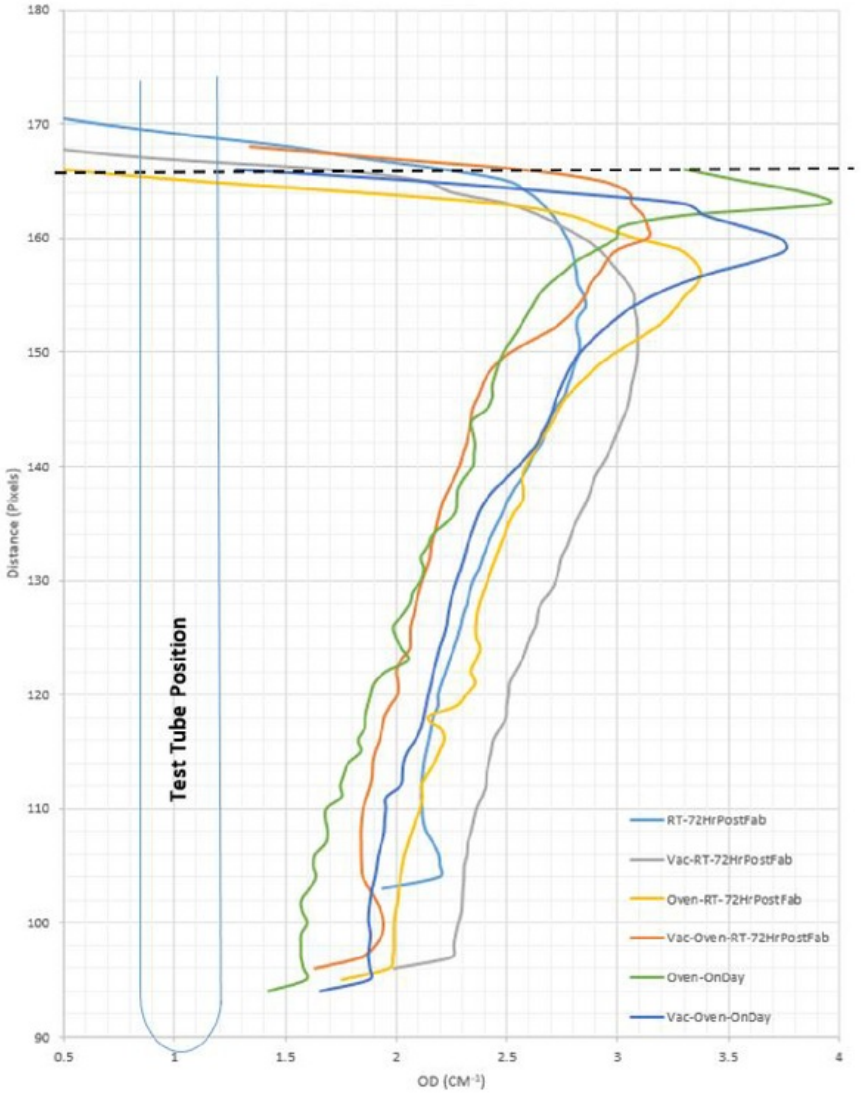

Figure 5.4: *The graph shows the resulting change in the OD profile over the length of the sample, for the upright position experiment. The OD profile is relative to the test tube. All six samples were cured using different procedures mentioned in table 4.3. Some samples had to be shortened as to fit within the field of view of the optical scanner. This can be observed at the start of the profiles (the bottom end). The dashed line indicates the actual end of all the samples, situated at the distance of 166 pixels.*

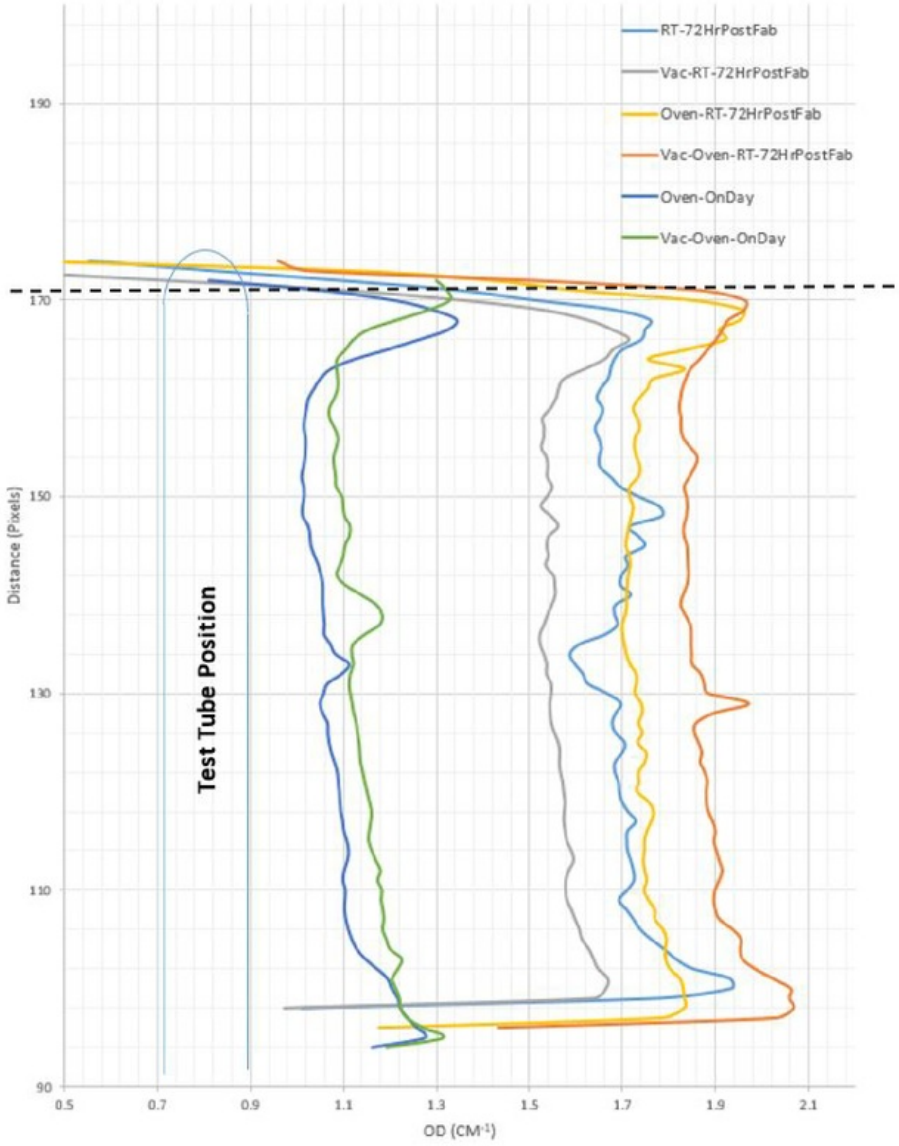

Figure 5.5: *The graph shows the resulting change in the OD profile over the length of the sample, for the downright position experiment. The OD profile is relative to the test tube. All six samples were cured using different procedures mentioned in table 4.3. The dashed line indicates the actual end of all the samples, situated at the distance of 171 pixels.*

With all the upright position samples following a similar OD profile, and no large distinctions between one another, there is no evidence to suggest which curing procedures have more chloroform evaporating. It was also found that the downright position samples showed no correlation between the OD with or without being in a vacuum desiccator. However, there was a correlation between the OD and when curing the samples with the oven and when curing in room temperature. The samples which were exposed to UV radiation on the day of fabrication displayed a lower OD response when compared to the samples which were exposed 72hrs after. There was no difference in the shape of the downright position samples profiles seen in figure 5.5, meaning that the various methods used to cure only change the samples sensitivity towards UV radiation. Considering that the resulting OD profiles for the curing procedures, used for both the upright or downright position samples, did not coincide, a sound conclusion cannot be made to which sample had more chloroform evaporating.

Placing the samples in the downright position showed a different trend as to that when in the upright position. This is evident when comparing figures 5.5 and 5.4. It was expected that both experiments (upright and downright positions) had a resulting OD profile trend which was similar. This was not the case. The resulting OD profile for the upright position samples was increasing along the direction of exposure, while the downright position samples was flat, only slightly increasing at the end. This slight increase at the end of the downright position samples was due to the concave shape of the glass test tube, causing the UV radiation to converge and increase the OD at this region. These results do not prove that the heterogeneity in OD is attributed to non-uniformity of the UV radiation source or chemical processes within the samples. There is insufficient evidence to determine if chloroform is indeed evaporating from the FlexyDos3D elastomer.

5.3 Dependence of the Stability on Curing Agent

When using the SYLGARD® curing agent at 1-2% concentration, the FlexyDos3D elastomer did not fully cure. No results were gathered for the corresponding samples. The change in OD over time for curing agent concentrations 3-5% are shown in figure 5.6. Concentrations 7.5-15% are shown in appendix B.

Curing agent concentrations 3-4.5% shown in figure 5.6(a-c), proved to be far more stable than any other concentration used in FlexyDos3D. There is little to no change in the OD over the three days after exposure to UV radiation. It was observed that these curing agent concentrations in FlexyDos3D were both soft and tacky, even several days after fabrication.

At 3% curing agent concentration or below, the elastomer gel can no longer be used for practical applications. Its strength had greatly diminished, and would prove to be too difficult to handle. The ideal concentrations suitable for practical applications would be that of 4% and 4.5%. A large decrease in OD over time begins between 4.5-5% curing agent concentration, and continues to decrease significantly from 5% onwards. This is due to a large increase in chemical reactions, which has shown to cause instability and

subsequently a large decrease in OD.

This experiment also indirectly contributes to the chloroform evaporation experiment (section 4.2). The resulting change in OD graphs indicate there may not be any chloroform evaporation taking place. If it were so, then all curing agent concentrations would be expected to show a large decrease in OD over time. However, this was not evident in concentrations below 4.5%. It may be possible that a certain curing agent concentration range initiates chemical processes which counteract the potential chloroform evaporation. Further investigations are required to test this hypothesis.

Figure 5.7 investigated the correlation between the stability of FlexyDos3D and the various curing agent concentrations. The graph shows that there isnt a linear or exponential relationship across all the concentrations. However, certain sections in the graph do represent linear relationships. Concentrations 3-4.5% and 5-10% represent a linear relationship.

This investigation proved to be successful in finding a stable response in the OD at certain curing agent concentrations within FlexyDos3D. Curing agent concentrations 3-4.5% showed little to no decrease in the OD over three days, and proved to be the optimal range for a more stable FlexyDos3D. Concentrations from 4.5% and above do not, and greatly diminish the stability. For practical applications, it was found that concentrations between 4% and 4.5% are most suitable. Though they are relatively soft and tacky, they may still be used.

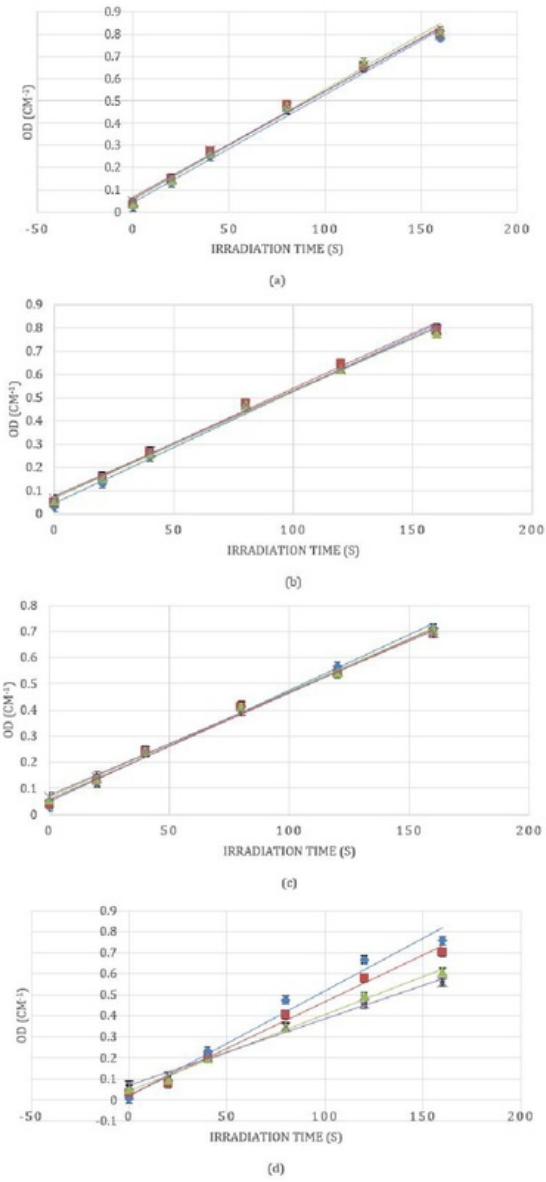

Figure 5.6: *All four graphs display the resulting change in OD at room temperatures for concentrations 3% (a), 4% (b), 4.5% (c), and 5% (d). This was over several irradiation times, on day 0 (blue), day 1 (red), day 2 (green), and day 3 (purple). A linear trendline was fitted across the different irradiated times of each day. Curing agent concentrations 3-4.5% show little to no decrease in OD over the three days.*

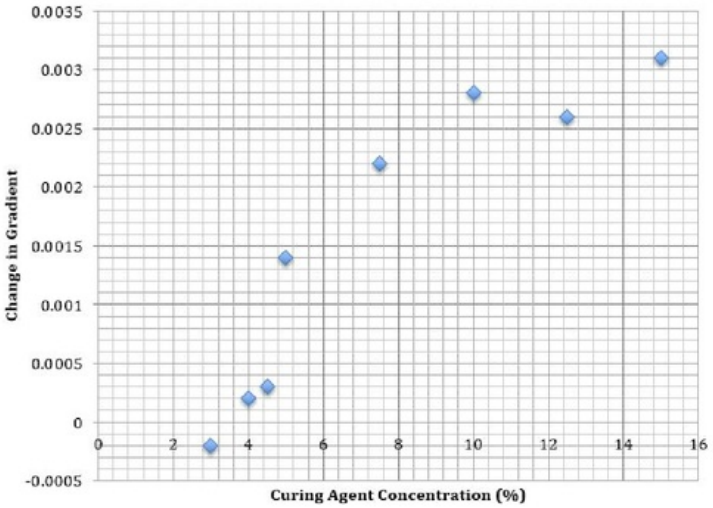

Figure 5.7: *The change in gradient over three days for the various curing agent concentrations tested. A large step can be seen between concentrations 4.5% and 5%, indicating the stability of FlexyDos3D begins to greatly diminish at these concentrations. At 3%, the change in gradient is observed to be negative, indicating the change in OD over several days doesnt decrease, but rather increases. There are no results for concentrations below 3%, as these samples did not cure at such low curing agent concentrations.*

5.4 3D Printing of Prostate Phantom

Figure 4.1 shows the 3D rendered mould of the prostate tumour in the Meshmixer software. Figure 5.8 shows the final 3D printed moulds.

When using the ABS material to 3D print the prostate tumour mould, it was found that the material did not adhere well to the platform of the Flashforge Dreamer printer. The base of the model slowly warped as the print progressed, which can be seen with the ABS material in figure 5.8. Various nozzle and platform temperatures were trialled, but there were no significant improvements.

A soluble filament was trialled to provide the supporting structures, but neither ABS or PLA adhered to it. This may be due to the required platform temperature of the soluble filament being far lower compared to that of ABS and PLA. For this reason, the soluble filament was not used, and no supporting structures were built for the prostate tumour mould. The mould was still printed well without the supporting structures, though there were a few defects present on the overhanging structures. These defects did not render the model unusable, but a supporting structure should be considered for future builds. There were far less issues when printing with PLA than ABS. PLA was found to have less defects and warping when compared to ABS; hence a more suitable material to 3D

print with using the Flashforge Dreamer printer.

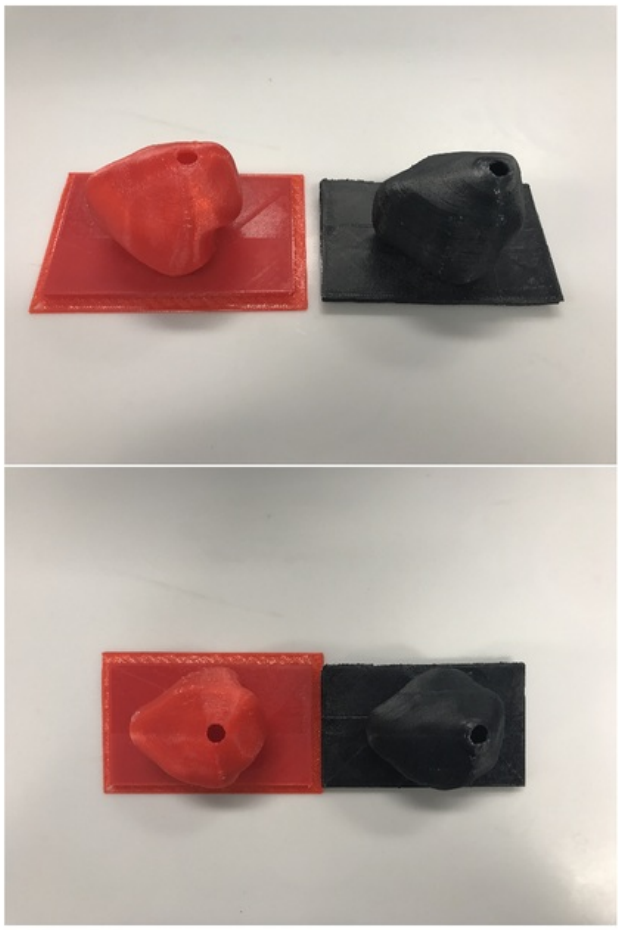

Figure 5.8: *The final 3D printed prostate tumour mould. The left mould (red) has been fabricated from PLA, while the right mould (black) fabricated from ABS. The ABS mould can be seen with more defects and warping of the baseplate.*

The prostate tumour mould was built best when using PLA, leaving little to no defects when using no supporting structures. The soluble filament was not used in any of the builds, due to its inability to adhere to PLA or ABS. However, future builds should utilise supporting structures to avoid any defects on overhanging features. The procedure for fabricating a 3D prostate tumour mould was found to be successful, and may be followed for all future builds.

5.5 Mechanical Properties

A few of the samples had defects (air bubbles) when fabricated, causing the sample to fail earlier than expected. The samples that had a defect were the 5% Day 0 and 4% Day 3. They can be seen in figure 5.9 by discontinuing at an early stage, indicating failure.

The 5% Day 3 sample can be seen to have the highest strain than any other sample. This was assumed, as using the curing agent at 5% concentration provided a far stiffer FlexyDos3D sample. What was irregular in figure 5.9, is that 5% Day 3 did not follow a smooth curve, but rather had several steps. The samples were far too soft to be clamped tightly by the grips on either side, as this clamped region would create too much stress. This caused the sample to break at the grip rather than the gauge section. For this reason, the samples were gripped loosely, which caused slipping in some cases. The steps in the 5% Day 3 samples were due to slight slipping and repositioning of the sample when testing.

There is a reasonable improvement in Youngs Modulus between the samples tested on Day 0 and those on Day 3. This suggests that either the samples were still curing over time, or chemical processes continue to occur due to the additives within FlexyDos3D. The 4% Day 0 sample had a far lower Youngs Modulus than any other concentration, and this may be due to the sample not being cured completely. It was difficult to distinguish if this was true when removing from the oven as all the samples remained soft and tacky.

An unexpected result was shown with the 4.5% Day 0 sample having a higher Youngs Modulus than that of 5% Day 0. However, this was not evident after three days. The reason remains unknown, but may be an anomaly. Further investigations are required.

This experiment has provided quantitative results for Youngs Modulus and UTS of various curing agent concentrations within FlexyDos3D. However, due to the experimental discrepancy of the specimens slipping, the results found in this experiment shouldn't be considered exact. Rather, this experiment has provided a rough insight into the Youngs Modulus and UTS values for the various curing agent concentrations. These values may be used for rough estimates in future experiments and applications. For a more accurate set of results, this experiment should be repeated.

Table 5.1: The Youngs Modulus and UTS for all the tensile tested samples, seen in figure 5.9

Sample	Youngs Modulus (KPa)	UTS (KPa)
4% Day 0	32.77	50
4.5% Day 0	90.39	93
5% Day 0	70.39	55
4% Day 3	115.52	110
4.5% Day 3	152.12	140
5% Day 3	186.68	168

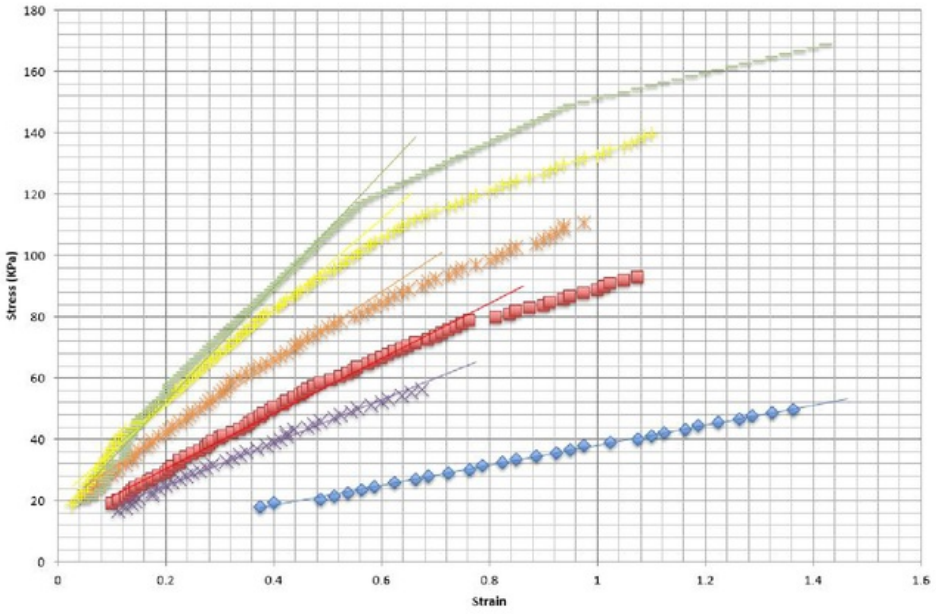

Figure 5.9: *The Stress Vs Strain graph for the various curing agent concentrations that underwent tensile testing: Blue-4%Day0, purple-5%Day0, red-4.5%Day0, orange-4%Day3, yellow-4.5%Day3, and green-5%Day3*

Chapter 6

Conclusion and Future Work

With more attention directed towards a more accurate delivery of radiation, there has been a growing need for 3D radiation dosimeters to improve the quality of treatments. This study has successfully benchmarked the 3D radiation dosimeter in terms of its stability and temperature sensitivity. It has been found that using curing agent concentrations of 4-4.5% is most stable within FlexyDos3D. This displays little to no decrease in OD over several days, and is ideal for future applications. Furthermore, the 3D radiation dosimeter has been designed to be able to be reproduced (in terms of its shape), by the use of a 3D printer. By implementing this technique, a standard mould may be printed in which the FlexyDos3D elastomer gel may be poured into and take shape.

It was found that using dibromomethane as the initiator in FlexyDos3D, was not as suited as chloroform. Both displayed a similar response to UV radiation over time, and no significant improvement in the stability was seen. Both chloroform evaporation experiments (upright and downright position) were unsuccessful in concluding if chloroform was evaporating. Rather, evidence showed that various curing procedures either increased or decreased the sensitivity of FlexyDos3D. The mechanical properties of the various curing agent concentrations within FlexyDos3D were determined, but due to experimental errors and discrepancies, the results should only be used as rough estimates. To attain more accurate results, this experiment should be repeated.

Unfortunately due to limited time, utilising motion controlled 3D radiation dosimeters did not take place. Neither did irradiating the radiation dosimeters at the RNSH by the use of IMGRT. Overall, this study has been found to be successful in achieving the short-term goals of a more stable and reproducible FlexyDos3D radiation dosimeter. These improvements have taken the right step into achieving the goal of a standardised 3D dosimetry protocol for IMGRT to safeguard the radiotherapy treatment administrated for cancer patients.

Future works involve proceeding to implement the 3D prostate tumour moulds in a radiation treatment plan. This is by filling the moulds with the stable FlexyDos3D, attaching the mould to the Hexamotion, and irradiating at the RNSH by IMGRT. Future works also include investigations into determining the reasons for an unstable FlexyDos3D at curing agent concentrations above 4.5%. It may also be beneficial to study if a correlation exists between the curing agent concentration, and potential chloroform evaporation.

Chapter 7

Abbreviations

ABS	Acrylonitrile-Butadiene-Styrene
CCD	Charge Coupled Device
$CHCl_3$	Chloroform
CRT	Conformal Radiation Therapy
CT	Computed Tomography
CH_2Br_2	Dibromomethane
DMLC	Dynamic Multi-leaf Collimator
FXG	Fricke Xynlenol Gel
Hrs	Hours
IMAT	Intensity Modulated Arc Therapy
IMGRT	Image Guided Radiation Therapy
IMRT	Intensity Modulated Radiation Therapy
LMG	Leuco Malachite Green
Min	Minutes
MRI	Magnetic Resonance Imaging
NMR	Nuclear Magnetic Resonance
OD	Optical Density
PDMS	Polydimethylsiloxane
PLA	Polylactic Acid
PMMA	Polymethyl Methacrylate
RNSH	Royal North Shore Hospital
RT	Room Temperature
R_2	Spin-Spin Relaxation Rate
S	Seconds
SDS	Safety Data Sheet
UTS	Ultimate Tensile Strength
UV	Ultraviolet
VMAT	Volumetric Modulated Arc Therapy
2D	Two Dimensional
3D	Three Dimensional

Appendix A

Reconstruction of Irradiated Samples

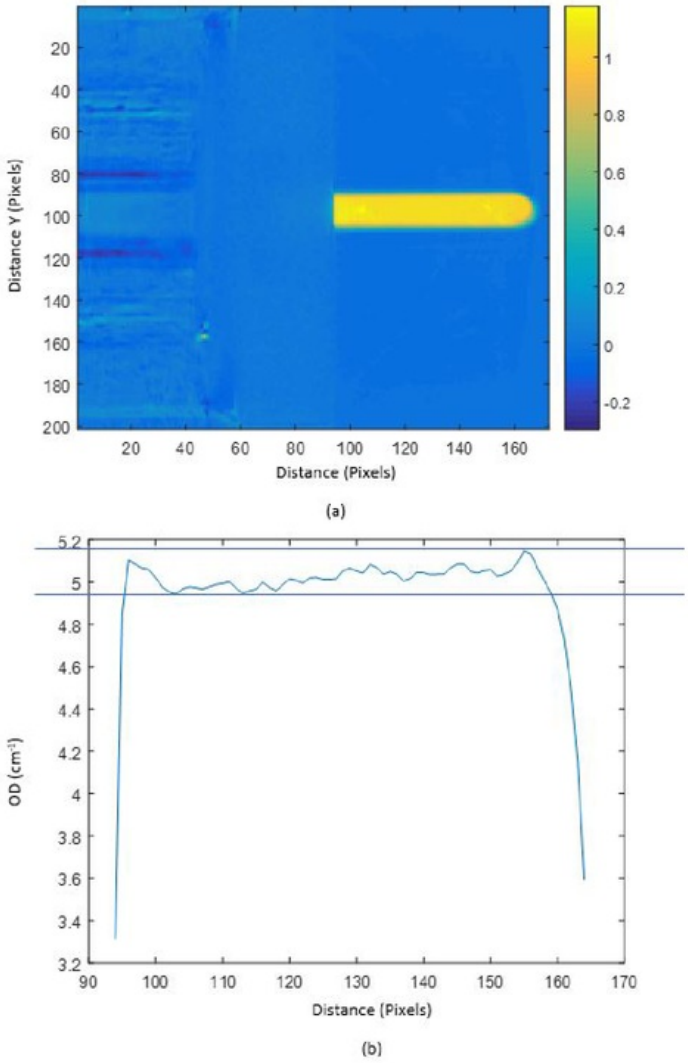

Figure A.1: *(a) The reconstructed image of the sample which had been irradiated for an extensive time before fabrication. The colour bar on the right hand side of image represents the OD. (b) Shows the change in OD over the samples length, where the variance in OD is noise. It is evident that the reconstruction process does not change the resulting OD in any significant way*

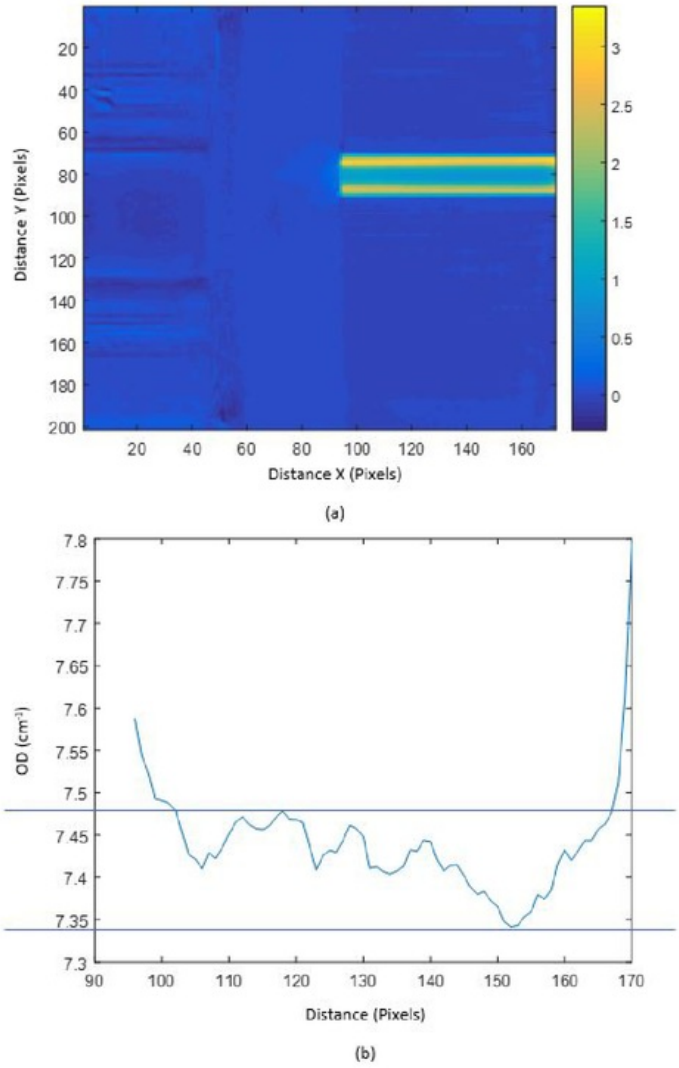

Figure A.2: *(a) The reconstructed image of the sample which had been irradiated for an extensive time after fabrication. Only the outer edges have responded, indicating the UV radiation did not penetrate the sample regardless of the time spent irradiating. The colour bar on the right hand side of image represents the OD. (b) Shows the change in OD over the samples length, where the variance in OD is noise. It is evident that the reconstruction process does not change the resulting OD in any significant way*

Appendix B

Curing Agent Concentrations 7.5-15%

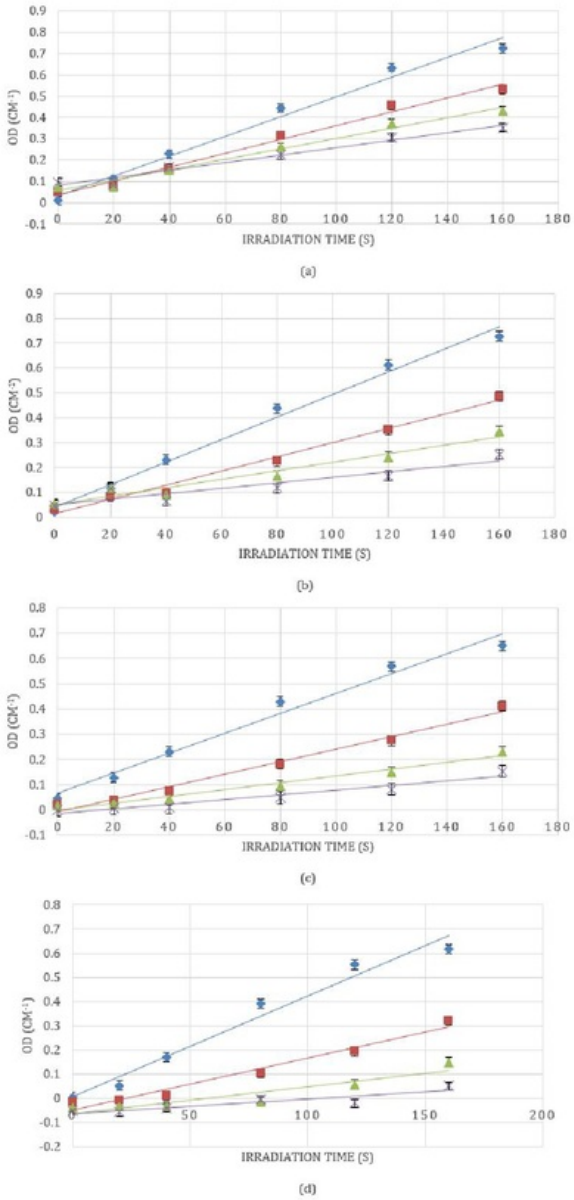

Figure B.1: *All four graphs display the resulting change in OD at room temperatures for concentrations 7.5% (a), 10% (b), 12.5% (c), and 15% (d). This was over several irradiation times, on day 0 (blue), day 1 (red), day 2 (green), and day 3 (purple). A linear trendline was fitted across the different irradiated times of each day.*

Appendix C

MATLAB Script

```
% selecting a slice
img = squeeze(Reconima(:,150,:));
%
figure(2);
imagesc(img)
%
% Spot the Region Of Interest
%The lenght of sample
xmin = 94;
xmax = 166;
xRange = xmin:1:xmax;
% first rectangle
ymin1 = 45;
ymax1 = 49;
% second rectangle
ymin2 = 55;
ymax2 = 59;
%
% Finding the average value across y dim
avg = zeros(xmax-xmin+1,1);
for i = xmin:xmax
    ysum = 0;
    yavg = 0;
    for j = ymin1:ymax1
        ysum = ysum + img(j,i);
    end
    for k = ymin2:ymax2
        ysum = ysum + img(k,i);
    end
    yavg = ysum/(length(ymax1-ymin1)+length(ymax2-ymin2));
    avg(i,1) = yavg;
end
%
avg(avg == 0) = [];
%
% plotting
figure(2);
plot(xRange,avg)
```

Figure C.1: *The MATLAB script used in selecting the regions of interest on image slice from the reconstructed images. The resultant figure is a graph displaying the change in OD over the length of the sample.*

Appendix D

Consultation Meeting Form

Consultation Meetings Attendance Form

Week	Date	Comments (if applicable)	Student's Signature	Supervisor's Signature
1	2/3/17	Introduction		
2	10/3/17	Optical Scanner Intro Chloroform Evap Exp		
3	16/3/17	Results Discussion Further Experiments		
4	24/3/17	Results Discussion Further Experiments		
6	07/4/17	Results Discussion Further Experiments		
7	13/4/17	Discussion		
Mid-Sem Break	21/4/17	Discussion		
Mid-Sem Break	28/4/17	Discussion Manufacturing Mould		
9	11/5/17	Results Discussion		
10	19/5/17	Results Discussion		
	-			

References

[1] Y. De Deene, "Safeguarding radiotherapy: Three dimensional radiation dosimetry," *Aus. Bio. Med. Conf*, 2014.

[2] C. Wuu, S. Hoogcarspel, K. Deh, W. Hsu, and J. Adamovics, "3-d dose verification by cone-beam optical ct scanning of presage dosimeter," in *7th International Conference on 3D Radiation Dosimetry.* Journal of Physics, 2013.

[3] C. Baldock, Y. De Deene, S. Doran, G. Ibbott, A. Jirasek, K. McAuley, M. Oldham, and L. Schreiner, "Polymer Gel Dosimetry [review]," *Phys. Med. Biol*, vol. 55(5), pp. R1–R65, 2010.

[4] P. Fong, D. Keil, M. Does, and J. Gore, "Polymer gels for magnetic resonance imaging of radiation dose distributions at normal room atmosphere," *Phys. Med. Biol.*, vol. 46, pp. 3105–13, 2001.

[5] Y. De Deene, C. De Wagter, B. Van Duyse, S. Derycke, W. De Neve, and E. Achten, "Three-dimensional dosimetry using polymer gel and magnetic resonance imaging applied to the verification of conformal radiation therapy in head-and-neck cancer," *Radiother. Oncol.*, vol. 48, pp. 283–91, 1998a.

[6] R. Senden, P. De Jean, K. McAuley, and L. Schreiner, "Polymer gel dosimeters with reduced toxicity: a preliminary investigation of the nmr and optical doseresponse using different monomers," *Phys. Med. Biol.*, vol. 51, pp. 3301–14, 2006.

[7] E. Bakiu, E. Telhaj, E. Kozma, F. Ruci, and P. Malkaj, "Comparison of 3d crt and imrt treatment plans," *Acta Inform Med*, vol. 21, no. 3, pp. 211–212, 2013.

[8] F. Sterzing, R. Engenhart-Cabillic, M. Flentje, and J. Debus, "Image-guided radiotherapy," *Dtsch Arztebl Int*, vol. 16, no. 108, pp. 274–80, 2011.

[9] E. Hoye, P. Balling, E. Yates, L. Muren, J. Petersen, and P. Skyt, "Eliminating the dose-rate effect in a radiochromic silicone-based 3d dosimeter," *Phys, Med. Biol*, vol. 60, pp. 5557–5570, 2015.

[10] S. Babic, J. Battista, and K. Jordan, "An apparent threshold dose response in ferrous xylenol-orange gel dosimeters when scanned with a yellow light source," *Phys. Med. Biol*, vol. 53, 2008.

[11] S. Cerberg, "3d verification of dynamic and breathing adapted radiotherapy using polymer gel dosimetry," *Ph.D Thesis, Dept. Clin. Sci, Lund Uni, Lund, Sweden*, 2010.

[12] N. Hanif, "Measuring radiation dose in the vicinity of prosthesis in cancer patients using a 3d radiation dosimeter," Master's thesis, Macquarie University, February 20 2016.

[13] Y. De Deene, "Flexydos3d: a deformable anthropomorphic 3d radiation dosimeter: radiation properties," *Phys. Med. Biol.*, vol. 60, pp. 1543–63, 2015.

[14] Y. De Deene, R. Hill, P. Skyt, and J. Booth, "Flexydos3d: A new deformable anthropomorphic 3d dosimeter readout with optical ct scanning," in *8th International Conference on 3D Radiation Dosimetry*, ser. 573. Journal of Physics, 2015.

[15] J. Gore, M. Ranade, M. Maryanski, and R. Schulz, "Radiation dose distributions in three dimensions from tomographic optical density scanning of polymer gels: I. development of an optical scanner." *Phys.Med Biol.*, vol. 41, pp. 2695–2705, 1996.

[16] J. Wolodzko, C. Marsden, and A. Appleby, "Ccd imaging for optical tomography of gel radiation dosimeters," *Med. Phys*, vol. 26, pp. 2508–213, 1999.

[17] S. Doran, K. Koerkamp, M. Bero, P. Jenneson, E. Morton, and W. Gilboy, "A ccd-based optical-ct scanner for high-resolution 3d-imaging of radiation dose distributions: equipment specifications, optical simulations and preliminary results," *Phys. Med. Biol.*, vol. 46, pp. 3191–213, 2001.

[18] U. Yeo, M. Taylor, L. Dunn, T. Kron, R. Smith, and R. Franich, "A novel methodology for 3d deformable dosimetry," *Med. Phys.*, vol. 39, pp. 2203–13, 2012.

[19] Y. De Deene, "Essential characteristics of polymer gel dosimeters," in *J.Phys: Conf*, ser. 3, 2004b, pp. 34–57.

[20] S. Burleson, J. Baker, A. Hsia, and Z. Xu, "Use of 3d printers to create a patient-specific 3d bolus for external beam therapy," *Med. Phys.*, vol. 16, no. 3, 2014.

[21] S. Park, C. Choi, J. Park, M. Chun, J. Han, and J. Kim, "A patient-specific polylactic acid bolus made by a 3d printer for breast cancer radiation therapy," *PLoS ONE*, vol. 12, no. 11, 2016.

[22] *Safety Data Sheet, Slygard(R) 184 Silicone Elastomer Kit*, Dow Corning, October 2016.